T

Theory of Nonionic Diffusion

► pH Partition Theory

Therapeutic Equivalence

► Bioequivalence

Therapeutic Target

► Pharmacodynamic Polymorphisms

Thin-Film Diffusion Models

► Drug Dissolution: Fundamental Theoretic Models

Time-Dependent Nonlinear Pharmacokinetics

Pietro Fagiolino and Manuel Ibarra
Department of Pharmaceutical Sciences, Universidad de la República, Montevideo, Uruguay

Synonyms

Pharmacokinetic response to drug action is not immediate; Delay between drug action, drug effect and final drug exposure

Relationship Between Dose and Drug Concentration

After administering a dose, the individual responds by absorbing and disposing the molecules there contained in such a way that body concentrations (C) will vary over time (t) until they are definitely eliminated from the body. This C(t) profile is known as the drug-individual system's pharmacokinetic (PK) response. That is, any action that the body performs on the administered molecules constitutes the PK response. On the other hand, drug molecules and/or their metabolites may act at the different sites of the body

A.Talevi (ed.), *The ADME Encyclopedia*,
https://doi.org/10.1007/978-3-030-84860-6

where action receptors are found and thus display what is known as the pharmacodynamic response (PD) of the system. More precisely, PD responses are the effects that directly derive from substrate actions on those receptors or the ones that are established because of the drug action and the individual reaction.

If the same individual received a higher dose, the PK response would be higher by virtue of the increased entry of molecules into the system. Therefore, the PK response of the system will always be higher as the dose increases. If such concentration increases are proportional to the dose increase, it will be said that the system responds linearly. Any departure from such proportionality characterizes the system as nonlinear. That is, the increase in concentrations could be higher or could be lower than expected after the dose increase. Nonlinear PK responses are always the result of a concentration dependency in either dose bioavailability or system clearance. In other words, either the arrival (bioavailability) to or the exit (clearance) from the site where the PK response is recorded could be governed by a concentration-dependent kinetics.

For single doses, the best way to quantify the PK response is by means of the area under the concentration-time curve (AUC):

$$AUC_{0\ single\ dose}^{\infty} = \frac{F \cdot dose}{CL} \tag{1}$$

where F is the fraction of dosage that enters the site where the concentrations are measured and CL is the elimination clearance from that site.

The site where the PK response has most often been measured is blood, especially its plasma fraction. However, from a therapeutic point of view, other more interesting sites to be monitored would be the extravascular ones, where the action receptors are mostly placed. Since the blood connects these extravascular sites, their F values take into account both the input to plasma and the input to the site where concentration is measured. In addition, CL from an extravascular site takes into account the return of drug to plasma, the output from plasma to the elimination site, and finally the output from there to the outside of the system.

The kinetics describing the transport between the different sites of the system can be described by the following equation:

$$\frac{dX(t)}{dt} = k \cdot X(t) = CL \cdot C(t) \tag{2}$$

where the amount of drug (X) is multiplied by the rate constant (k) to yield the velocity of the transfer process. Also, such transfer rate results from the product between clearance and concentration.

Equation 2 provides a proportionality between the transfer rate from the compartment where the process is measured and the amount or concentration of drug hosted there. At other times, mass transfers are adjusted to kinetics where the drug concentration itself also integrates the proportionality factor: k or CL. Although equations may vary in their degree of complexity, they could be simplified by the well-known Michaelis-Menten equation, both for enzyme biotransformations [1] and for transporter-mediated transferences across membranes [2]:

$$\frac{dX(t)}{dt} = \frac{V_{MAX} \cdot C(t)}{K_m + C(t)} \tag{3}$$

V_{MAX} being the maximum transfer rate and K_m the concentration at which the speed results in half of V_{MAX}.

When $C(t) << K_m$, the rate of the transfer process is manifested as first-order (Eq. 2) with $CL = {}^{V_{MAX}}/_{K_m}$. Instead, when $C(t) >> K_m$, the transfer kinetics becomes of zero order with $CL = {}^{V_{MAX}}/_{C(t)}$.

Therefore, some of the clearances that carry drugs out of the system may not be independent of concentration. It may also not be the case for the fraction of dose that comes from the absorption site, since such a fraction results from clearance ratios that compete both at the entrance to plasma and at the entrance to the monitoring site.

When the concentration-dependent kinetics shown in Eq. 3 governs such processes, PK responses are no longer linear. Very often at low doses, the system, in any of its compartments, will be in condition to respond linearly, since transfer kinetics are most likely all of first order. In contrast, as the dose increases, probably some of the

kinetics that define F or CL will depend on the concentration. If by chance such modifications in F and CL were compensated one to each other, the PK response would remain linear. Conversely, an increase in the F/CL ratio leads to a larger increase, while a decrease in the quotient leads to a smaller increase than that proportionally foreseen by the dose increase.

As Eq. 3 shows, the inconstancy of clearance is also time-dependent since the concentration is not constant over time. However, it must be pointed out that the nonlinear PK response is not because of the variable exposure over time but because of the total drug exposure, which is recorded by the $AUC_{0\text{-inf}}$ whose metric is not time-dependent.

In short, it would be more appropriate to say that a nonlinear PK response is the result of some concentration-dependent clearance throughout the path that goes from the absorption site to the elimination site, passing through the site where the response is being monitored.

Constant Systems and Variant Systems

Drug concentrations referred at the end of the previous section could modify the clearance in a passive or active manner. To understand this point, it is necessary to distinguish two different situations: (1) the individual acts according to its intrinsic capacities for absorbing and disposing the drug; (2) the individual modifies such capabilities by effect of an action that the drug itself performs on it.

In the first case, there are no biochemical changes in the system every time the dose increases. This produces passive increases in concentrations along the different compartments of the system modifying, or not, any of the clearances referred to in the final paragraph of the previous section (nonlinear or linear PK response, respectively).

In the second case, however, the concentrations achieved after dose increases exceed action thresholds on certain biological receptors, the effects of which could change the kinetics of absorption and/or disposition of the drug. These PD responses have not been usually referred to as such, but in reality they are since the drug acts on the body. They have the peculiarity of modifying the physiology of the individual in such a way that the intrinsic constants of the transfer processes described by Eqs. 2 and 3 (k, V_{MAX}, K_m) are ultimately affected. Some of these effects are the induction [3] and inhibition [4] of transporters and enzymes, modification of the vascular caliber with alteration of the cardiac output distribution [5], etc. In short, a PK response that could initially be carried linearly or nonlinearly, as would occur in a constant system, might become nonlinear or linear, respectively, because of the drug action. Dosage-dependent, and therefore concentration-dependent, variant systems can sometimes lead to unsuspected changes in their PK responses, as will be exemplified with phenytoin, a recognized antiepileptic drug and at the same time inducer of the metabolism of drugs.

Since concentrations are first reached after a dose is administered, which then triggers PD responses, which in turn modify the initial PK response, it is reasonable to wait a certain time before the final PK response can be appreciated. This sequence gives name to the time-dependent PK response, which is actually always concentration-dependent only that it takes a while to see the result, sometimes too long to be appreciated after a single dose.

Pharmacokinetic Response After Multiple Dose

Because the transformation of the system takes a while to consolidate and since most drugs are chronically administered for the purposes of achieving their therapeutic benefits, it is therefore more convenient to characterize the PK response by determining the concentrations at the steady state of multiple dose. Equation 1 will then be expressed as follows:

$$AUC^{\tau}_{0\ steady\ state\ of\ multiple\ dose} = \frac{F \cdot dose}{CL} = C_{ss\ avetage} \cdot \tau \tag{4}$$

where τ is the interval during which the concentrations acquire a steady-state C(t) profile that will

T

be repeated successively, while the same dosage schedule is kept. $C_{ss\ average}$ is the mean concentration within such interval τ. The same arguments already discussed under single-dose administration are those that define now whether a PK response is linear (constant F/CL) or nonlinear (F/CL variant) with respect to the dose (administration rate, dose/τ, under multiple doses). No matter how long it takes for the transformation of the system, consolidation of the new system will always have been fulfilled once the steady state is reached.

Many drugs transform the system progressively over the course of the first dosing plan. Inducers of the expression of enzymes and membrane transporters have PK responses that vary from the first to the nth administration by virtue of processing the biological changes that happen during that time, which follow the evolution of drug concentration at the sites of actions [6]. Also, drugs that act by inhibiting the expression of enzymes and/or transporters progressively transform the system during the establishment of the first dosing plan [7]. This explains the change in elimination half-life between the first dose and the umpteenth dose when the steady state is reached.

In constant systems, there could also be a progressive adaptation of the PK response during the first dosing plan, but in this case it is not due to the time that the pharmacodynamic action of the drug would entail but to the competition that the drug and its metabolites could have in its unions with different sites of the organism. Chemical similarity between drugs and metabolites could lead to a drug-metabolite interaction that would modify the binding of the administered drug to transporters and enzymes [8]. Very dissimilar half-lives between the first dose and after reaching the steady state of multiple doses could be due to the competitive inhibition that the metabolites would exert on the metabolism of their precursor. This would be a valid hypothesis to explain the considerable increase in the half-life of amiodarone elimination [9]. This is possible as metabolites slowly form and take time to achieve concentrations that can effectively compete with the precursor drug.

Phenytoin: A Paradigmatic Example of Nonlinear Response

This important antiepileptic drug was always used as an example of a nonlinear PK response, whose plasma concentration increases were more than proportional with respect to the administration rate increase. The most common explanation was that it possessed a concentration-dependent elimination of type Michaelis-Menten. However, this mechanism has been questioned recently. Here below, the main arguments will be summarized.

First, single oral doses between 100 and 300 mg phenytoin produced a linear PK response, with decreased absorption rate as the dose increased but not the amount absorbed [10]. That is, the $AUC_{0\text{-}inf}$ of plasma concentrations were proportionate to the doses received, keeping the elimination half-life constant (12–13 hr). Doses between 400 and 1600 mg showed progressive loss of bioavailability due to incomplete dissolution in the digestive tract [11]. The delay in reaching the maximum plasma concentration (C_{MAX}) when 1600 mg was administered was especially evident. However, when the dose was fractioned in 400 mg every 3 hr, the observed linear response at low doses was recovered for both $AUC_{0\text{-}inf}$ and C_{MAX}.

Second, the Michaelis-Menten kinetics observed after multiple dose administration [12] has been explained by a limited capacity of the enzymes in charge to metabolize the drug (CYP2C9 and CYP2C19).

Third, to more accurately estimate the systemic clearance according to Eq. 3, and hence K_m and V_{MAX} values, 15 mg/kg (approximately 1200 mg) was given intravenously [11], observing the typical negative concavity during the decay of phenytoin plasma concentrations, different from the positive one when a first-order kinetics applies. However, this negative concavity in the decay of plasma concentrations might not be due to a Michaelis-Menten kinetics but the masking of drug reabsorption following its secretion toward the intestinal lumen. Plasma profiles with secondary peaks after intravenous administration of phenytoin gave strong evidences of blood-

gastrointestinal recycling [13, 14]. Proof thereof is the fact that phenytoin poisoning was successfully resolved by oral administration of activated charcoal [15], proving to be an efficient mechanism to reduce its plasma exposure and to increase its systemic depuration [16].

Fourth, an alternative explanation for the increase in the rate of elimination after the intravenous dose of phenytoin (negative concavity for the concentration decay) could be made based on its capacity of inducing different enzymes, including those of its own metabolism [17]. However, this hypothesis must be ruled out because after multiple dose administration it accumulates more than expected and not less, as it should be if enzymatic induction was the cause of the nonlinear pharmacokinetics of this drug.

Because of the above inconsistencies, a hypothesis has been proposed [18] related to its inductive capacity not only at the enzyme level but also at the level of the efflux transporters that govern its hepatobiliary transfer and its passage into intestinal lumen across the apical membrane of enterocytes [19].

Increased expression of efflux transporters opposes to the effect that the increased expression of the enzyme would have, thus avoiding the increase in clearance as the daily dose increases. This is because phenytoin molecules are diverted to a site (gut) where their elimination is less

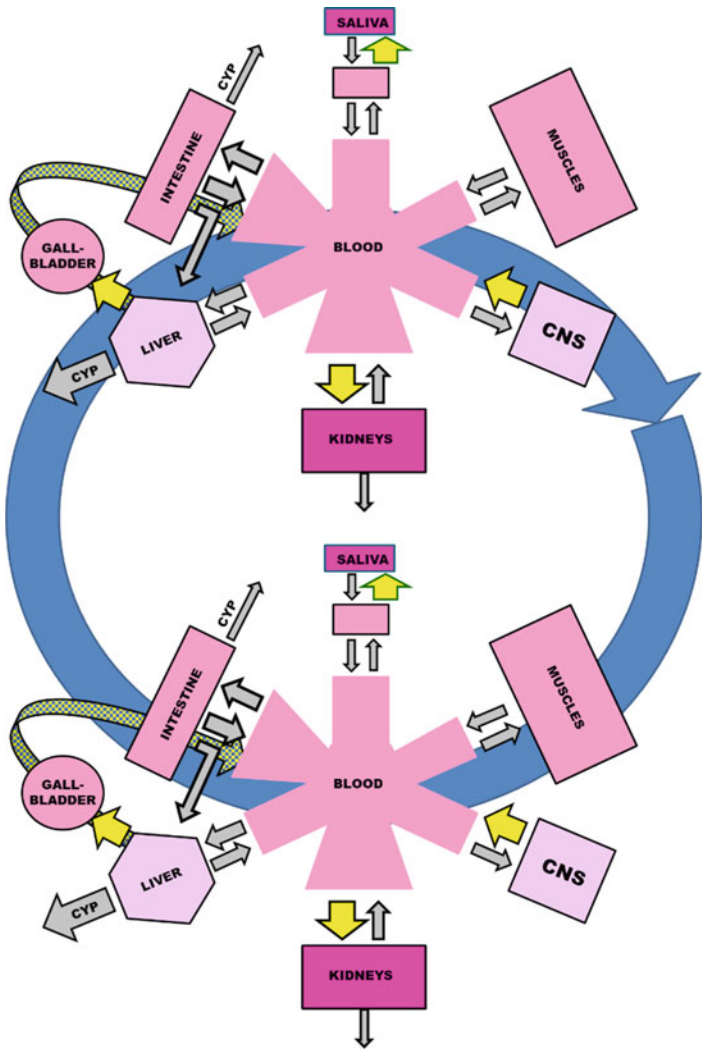

Time-Dependent Nonlinear Pharmacokinetics, Fig. 1 Phenytoin distribution among tissues following dosage schedules of 12-hr interval of dose. Yellow arrows stand for efflux transport. Compartment color intensity denotes relative concentration of drug. It can be noticed that CNS (brain)/blood ratio of free drug concentration is lower than one

intense than in the liver. Despite increased expression of CYP2C9 at the intestinal level, it is not enough to compensate for the sharp drop in liver metabolism.

In this way, the system changes after each daily dose change, requiring latency of at least 48 hr [6, 20] so that the intrinsic constant that carries the drug from the hepatocytes to the intestinal lumen could take the effect of reducing the hepatic clearance.

The opposite occurs in carbamazepine, which causes a transposition of its molecules from the liver to the intestine, organs that share in a similar proportion the elimination of the drug, and thus the net effect of its inductive action on transporters and enzymes leads to an increase in clearance with the increase of the daily dose [21].

Therapeutic Implications of the Nonlinear Phenytoin Response

The inductive effect on membrane transporters is not limited to the splanchnic region; also its expression is increased at the level of all the membranes that drive the substrates from the inside of vital organs (e.g., blood-brain barrier) to the outside of our body (apical membranes of digestive and renal mucosa). For this reason, antiepileptic drugs that have the property of inducing the expression of efflux transporters reduce their penetration into the brain as the daily dose increases. It is not surprising then that there are frequent cases of drug resistance in the treatment of epilepsy, partly induced by the same antiepileptic agent [22]. For phenytoin, an increase

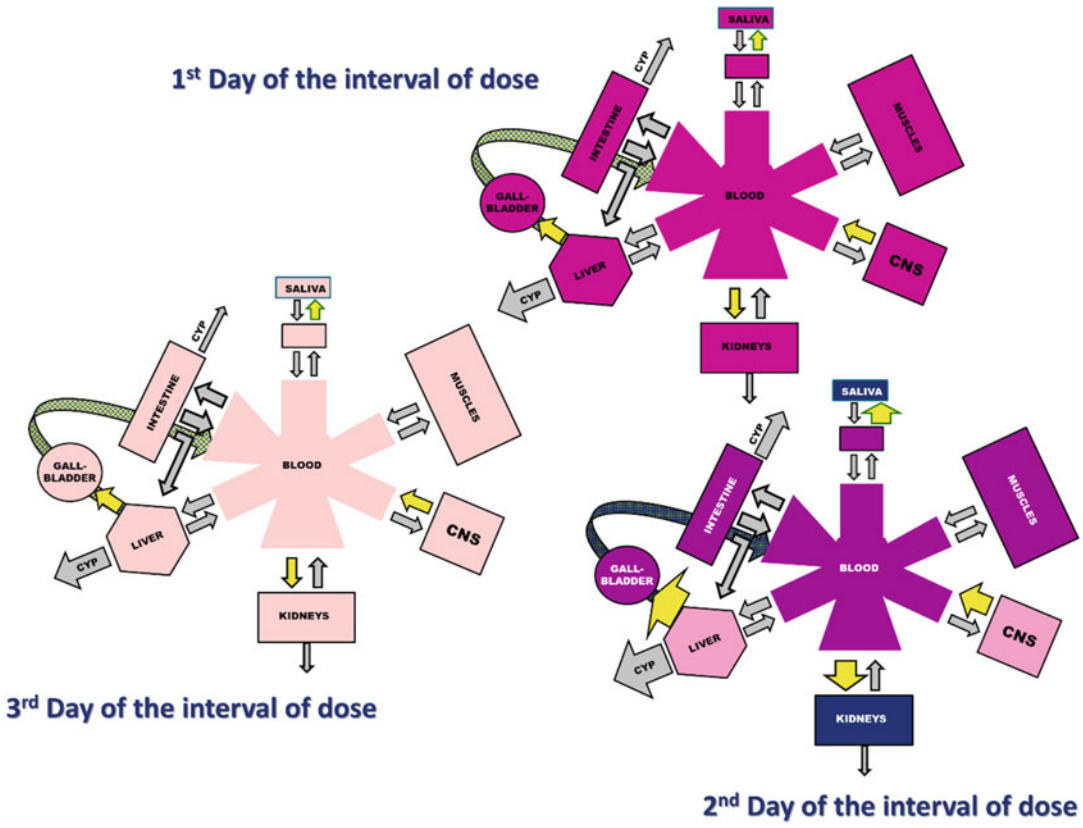

Time-Dependent Nonlinear Pharmacokinetics, Fig. 2 Phenytoin distribution among tissues following dosage schedules of 72-hr interval of dose. Yellow arrows stand for efflux transport. Compartment color intensity denotes relative concentration of drug. It can be noticed that efflux transporter expression and CNS (brain)/blood ratio of free drug concentration change throughout the interval of dose

in plasma concentrations by a greater proportion than the daily dose increase may not correspond to the increase in its brain concentration, where perhaps it was linear to or even less than the dose increase. Figure 1 shows, for the steady state of a regular twice-daily dosing schedule, a central nervous system-to-plasma free concentration ratio lower than one. This quotient could continue to decline if the dose were increased.

A relevant fact is that just as the induction of transporters and enzymes takes a while of being expressed, the removal of such inducer concentration lasts a similar period of time for recovering the previous expression level [19]. This led to suggest a dosage scheme where higher doses would be delivered at more spaced intervals without changing in the administration rate. In this way, the doses would find the system in a state of low protein expression and therefore more prone to allow the drug can penetrate the blood-brain barrier and reach its receptors of action more efficiently [22, 23]. Figure 2 illustrates the case of one bigger dose every 3 days, maintaining the same administration rate as the one depicted in Fig. 1.

It is important to bear in mind that the expression of enzymes and transporters vary throughout the interval of administration not only in those tissues relevant for clearing the drug (liver and intestine) but also in tissues where the sites of action are located. The same enzymes found in the liver also exist at the brain level [24, 25]. There is currently greater recognition of the role these enzymes would have in the duration of pharmacological action. In this sense, the inducer antiepileptic drugs could even reduce its concentration at the site of action as the dosing rate increases.

References

1. Schnell S. Validity of the Michaelis–Menten equation – steady-state or reactant stationary assumption: that is the question. FEBS J. 2014;281:464–72. https://doi.org/10.1111/febs.12564.
2. Tran TT, Mittal A, Aldinger T, Polli JW, Ayrton A, Ellens H, Bentz J. The elementary mass action rate constants of P-gp transport for a confluent monolayer of MDCKII-hMDR1 cells. Biophys J. 2005;88:715–38. https://doi.org/10.1529/biophysj.104.045633.
3. Gerk PM, Vore M. Regulation of expression of the multidrug resistance associated protein 2 (MRP2) and its role in drug disposition. J Pharmacol Exp Ther. 2002;302:407–15. https://doi.org/10.1124/jpet.102.035014.
4. Hu HF, Slater A, Wall DM, Parkin JD, Kantharidis P, Zalcberg JR. Cyclosporin a and PSC 833 prevent up-regulation of MDR1 expression by anthracyclines in a human multidrug-resistant cell line. Clin Cancer Res. 1996;2:713–20.
5. Fagiolino P, Eiraldi R, Vázquez M. The influence of cardiovascular physiology on dose/pharmacokinetic and pharmacokinetic/Pharmacodynamic relationships. Clin Pharmacokinet. 2006;45:433–48. https://doi.org/10.2165/00003088-200645050-00001.
6. Maldonado C, Fagiolino P, Vázquez M, Eiraldi R, Alvariza S, Bentancur C, Álvarez P. Time-dependent and concentration-dependent upregulation of carbamazepine efflux transporter. A preliminary assessment from salivary drug monitoring. Lat Am J Pharm. 2011;30:908–12. http://sedici.unlp.edu.ar/handle/10915/8235
7. Eiraldi R, Vázquez M, Fagiolino P, Fernández Lastra C, Mariño EL. Blood flow redistribution during renal posttransplant period and its impact on cyclosporine concentration. Lat Am J Pharm. 2008;27:354–9.
8. Tsao SC, Dickinson TH, Abernethy DR. Metabolite inhibition of parent drug biotransformation. Studies of diltiazem. Drug Metab Dispos. 1990;18:180–2.
9. Templeton IE, Chen Y, Mao J, Lin J, Yu H, Peters S, Shebley M, Varma MV. Quantitative prediction of drug–drug interactions involving inhibitory metabolites in drug development: how can physiologically-based pharmacokinetic modeling help? CPT Pharmacometrics Syst Pharmacol. 2016;5:505–15. https://doi.org/10.1002/psp4.12110.
10. Rojanasthien N, Chaichana N, Teekachunhatean S, Kumsorn B, Sangdee C, Chankrachang S. Effect of doses on the bioavailability of phenytoin from a prompt-release and an extended-release preparation: single dose study. J Med Assoc Thail. 2007;90:1883–93. http://www.medassocthai.org/journal
11. Jung D, Powell JR, Walson P, Perrier D. Effect of dose on phenytoin absorption. Clin Pharmacol Ther. 1980;28:479–85. https://doi.org/10.1038/clpt.1980.191.
12. Lin JH. Dose-dependent pharmacokinetics: experimental observations and theoretical considerations. Biopharm Drug Dispos. 1994;15:1–31. https://doi.org/10.1002/bdd.2510150102.
13. Handley AJ. Phenytoin tolerance tests. Br Med J. 1970;3:203–4. https://doi.org/10.1136/bmj.3.5716.203.
14. Glick TH, Workman TP, Gaufberg SV. Preventing phenytoin intoxication: safer use of a familiar anticonvulsant. J Fam Pract. 2004;53:197–202.

15. Howard CE, Roberts RS, Ely DS, Moye RA. Use of multiple-dose activated charcoal in phenytoin toxicity. Ann Pharmacother. 1994;28:201–3. https://doi.org/10.1177/106002809402800210.
16. Mauro LS, Mauro VF, Brown DL, Somani P. Enhancement of phenytoin elimination by multiple-dose activated charcoal. Ann Emerg Med. 1987;16:1132–5. https://doi.org/10.1016/S0196-0644(87)80471-7.
17. Brodie MJ, Mintzer S, Pack AM, Gidal BE, Vecht CJ, Schmidt D. Enzyme induction with antiepileptic drugs: cause for concern? Epilepsia. 2013;54:11–27. https://doi.org/10.1111/j.1528-1167.2012.03671.x.
18. Fagiolino P, Vázquez M, Eiraldi R, Maldonado C, Scaramelli A. Efflux transporter influence on drug metabolism: theoretical approach for bioavailability and clearance prediction. Clin Pharmacokinet. 2011;50:75–80. https://doi.org/10.2165/11539230-000000000-00000.
19. Alvariza S, Orozco-Suárez S, Feria-Romero I, Vázquez M, Fagiolino P. Chronic administration of phenytoin induces efflux transporter overexpression in rats. Pharmacol Rep. 2014;66:946–51. https://doi.org/10.1016/j.pharep.2014.06.007.
20. Alvariza S, Fagiolino P, Vázquez M, Rosillo de la Torre A, Orozco-Suárez S, Rocha L. Verapamil effect on phenytoin pharmacokinetics in rats. Epilepsy Res. 2013;107:51–5. https://doi.org/10.1016/j.epilepsyres.2013.09.001.
21. Fagiolino P, Vázquez M, Alvariza S, Maldonado C, Ibarra M, Olano I. Antiepileptic drugs: Energy-consuming processes governing drug disposition. Front Biosci. (Elite Edition). 2014;6:387–96. https://doi.org/10.2741/e714.
22. Fagiolino P, Vázquez M, Orozco-Suárez S, Maldonado C, Alvariza S, Feria I, Ibarra M, Rocha L. Contribution of the antiepileptic drug administration regime in the development and/or establishment of pharmacoresistant epilepsy. In: Rocha L, Cavaleheiro EA, editors. Pharmacoresistance in epilepsy: from genes and molecules to promising therapies. New York, Heidelberg, Dordrecht, London: Springer Science + Business Media, LLC; 2013. p. 169–84. https://doi.org/10.1007/978-1-4614-6464-8_11.
23. Fagiolino P, Vázquez M, Ibarra M, Maldonado C, Alvariza S. The actual mechanism by which phenytoin displays Michaelis-Menten kinetics. Epilepsia. 2017;58(Suppl. 5):S50. https://doi.org/10.1111/epi.13944.
24. Ferguson CS, Tyndale RF. Cytochromes P450 in the brain: emerging evidence for biological significance. Trends Pharmacol Sci. 2011;32:708–14. https://doi.org/10.1016/j.tips.2011.08.005.
25. Gerth K, Kodidela S, Mahon M, Haque S, Verma N, Kumar S. Circulating extracellular vesicles containing xenobiotic metabolizing CYP enzymes and their potential roles in extrahepatic cells via cell–cell interactions. Int J Mol Sci. 2019;20:6178. (18 pages). https://doi.org/10.3390/ijms20246178.

Total Brain-to-Plasma Ratio

▶ Brain-to-Plasma Concentration Ratio and Unbound Partition Coefficient

Total Clearance

▶ Total Clearance and Organ Clearance

Total Clearance and Organ Clearance

Alan Talevi[1,2] and Carolina L. Bellera[1,3]
[1]Laboratory of Bioactive Research and Development (LIDeB), Department of Biological Sciences, University of La Plata (UNLP), La Plata, Buenos Aires, Argentina
[2]Argentinean National Council of Scientific and Technical Research (CONICET) – CCT, La Plata, Buenos Aires, Argentina
[3]Consejo Nacional de Investigaciones Científicas y Técnicas (CONICET), La Plata, Buenos Aires, Argentina

Synonyms

Drug clearance; Hepatic clearance; Metabolic clearance; Organ clearance; Partial clearance; Renal clearance; Systemic clearance; Total clearance; Drug elimination

Definition

Clearance (*CL*) is one of the most relevant pharmacokinetic (PK) parameters to consider in both drug discovery and the clinical practice. It measures the ability of a living organism or a specific organ to eliminate a drug [1]. *Total* or *systemic clearance* reflects the overall ability of the organism (i.e., a pool of organs and tissues) to irreversibly remove a given chemical (without

distinguishing, in principle, which organ(s) or elimination route(s) contribute to such elimination). The total ability of the organism to eliminate a drug is given by the sum of hepatic clearance plus renal clearance (the primary sites where drugs are removed from the body) plus clearance by all other tissues [2]. *Partial clearance* refers to the removal of drug by a particular organ (*organ clearance*, e.g., *hepatic clearance* - CL_H, *renal clearance* CL_R) or a specific route of elimination (e.g., partial clearance by hydroxylation, N-oxidation). Generally, partial clearances relate to the total clearance additively [3]. For instance, if a drug is eliminated only through hepatic and renal elimination, the total clearance will correspond to the sum of CL_H and CL_R. The concept of clearance additivity is valid only when elimination organs receive their blood supplies in parallel (e.g., precisely, in the case of the kidneys and the liver). However, when the elimination organs elimination receive their blood supplies serially, such as pulmonary clearance in relationship to renal or hepatic clearance, the equations describing the relationship between systemic and organ clearances get more complicated.

CL reflects the apparent volume of a biological matrix (typically plasma or blood) that is completely cleared from drug per unit time. It is expressed in units of volume per time. Plasma clearance (CL_p) is the term most generally used, since plasma is the most used matrix to measure circulating drug concentrations [1]. If, instead of plasma drug levels, blood drug levels are measured, the blood clearance (CL_b) will be computed. If the drug concentrations in plasma and blood were identical, CL_p and CL_b would have the same numerical value [2, 4].

Analogously, the clearance of an eliminating organ can be defined as the volume of perfusing medium that is effectively cleared of drug by that organ per unit time (blood being usually the perfusing medium) [3].

CL_p could be computed as the (instantaneous) rate at which the drug is removed from plasma divided by the concentration of that drug in the plasma:

$$CL_p = \frac{rate\ of\ elimination}{C_p} = \frac{\frac{dA_e}{dt}}{C_p} \qquad (1)$$

where Cp denotes the plasma drug concentration and A_e symbolizes the amount of drug that has been eliminated. Note that while *CL* is typically constant (assuming linear elimination kinetics), the rate of drug elimination is concentration- (and thus time-) dependent. Since under linear kinetics *CL* is constant, this parameter says nothing, *per se*, about the mass of drug eliminated per unit time [3].

Also note that, in the context of the simplest PK model, the one-compartment model, and under a first-order elimination assumption, the rate of elimination can be written as $k_{el}\,A$, that is, the product of the elimination rate constant and the total amount of drug in the single compartment that represents the organism. Thus:

$$CL_p = \frac{k_{el} \cdot A}{C_p} \qquad (2)$$

Bearing in mind that in the framework of the one-compartment model, the total amount of drug in the compartment can be rewritten as the product of C_p and the apparent volume of distribution *V*, then:

$$CL_p = \frac{k_{el} \cdot V \cdot C_p}{C_p} = k_{el} \cdot V \qquad (3)$$

which confirms that, under the linear kinetics assumption, CL_p is constant (i.e., independent of the total amount of drug remaining in the body).

Total clearance can be estimated with relatively ease from plasma concentration-time curves, either through model-dependent approaches (classic compartmental models or physiologically based PK models) or using model-independent approaches (see entries on ▶ "One-Compartment Pharmacokinetic Model", ▶ "Two-Compartment Pharmacokinetic Model", ▶ "Physiologically Based Pharmacokinetic Modeling: Definition and History", and ▶ "Noncompartmental Pharmacokinetics"). Estimation of partial clearances, in contrast, requires the quantification of drug levels in specific sites of drug elimination.

As a matter of fact, CL_p could be regarded as the proportionality factor that relates the total area under the plasma drug concentration versus time

T

profile $AUC_{0\text{-}\infty}$ and the overall extent of drug exposure (i.e., the fraction of the administered dose that has become systemically bioavailable). For an intravenous bolus, for which the full dose D is bioavailable:

$$D = CL_p \cdot AUC_{0-\infty} \tag{4}$$

More generally, for any route of administration:

$$F \cdot D = CL_p \cdot AUC_{0-\infty} \tag{5}$$

where F is the fraction of the administered dose that is absorbed and reaches systemic circulation (unchanged), which equals 1 for the intravenous route. It follows that:

$$CL_p = \frac{F \cdot D}{AUC_{0-\infty}} \tag{6}$$

Since for an intravenous dose F equals 1, CL_p can be easily estimated by measuring the total area under the concentration-time curve. Alternatively, when administering the drug by intravenous infusion, CL_p can be assessed as:

$$CL_p = \frac{K_0}{C_{p\ ss}} \tag{7}$$

Here K_0 is the infusion rate and $C_{p\ ss}$ denotes the steady-state plasma concentration.

Relationship Between Blood Clearance and Plasma Clearance

Usually, clearance is designated by referring to the body fluid in which drug concentrations are measured. As previously mentioned, systemic clearance could be then referred as blood clearance or plasma clearance, depending on whether the drug levels are quantified in blood or plasma, respectively. For most drugs, the analytical matrix used is plasma; accordingly, plasma clearance is most frequently estimated.

Depending upon the blood-to-plasma ratio of the drug R_b [5] (i.e., the ratio between the whole blood-blood cells plus plasma-drug concentration of the compound and its plasma concentration), clearance can have different values when measured in plasma or blood [4]. Equation (8) provides the relationship between CL_p and CL_b:

$$CL_b = \frac{CL_p}{R_b} \tag{8}$$

when R_b is unity (the drug distributes uniformly between blood cells and plasma), and CL_p and CL_b will have identical numerical values.

Certain drugs can specifically bind to components within blood cells (e.g., erythrocytes), leading to high R_bs (above 1). For such drugs, CL_p significantly overestimates CL_b, and blood could be a more appropriate matrix to measure this parameter. Contrariwise, drugs that are preferably distributed to plasma (rather than blood) due to a high fraction bound to plasma proteins will likely have low R_bs, as these will approach the hematocrit, resulting in CL_b up to about twofold higher than CL_p [4].

Hepatic Clearance

Several physiological models of hepatic clearance have been reported which simplify the process of drug extraction by the liver in varying degrees (for more details on the physiology of hepatic clearance, the reader is referred to the entry on ▶ "Drug Excretion" and ▶ "Biliary Drug Excretion"). Among them, the *well-stirred model* has proven to be widely relevant, possibly being the most commonly used among the available models [4]. It depicts the liver as a single, well-stirred compartment (Fig. 1) so that the concentration of *unbound* drug in the blood that exits the organ is in equilibrium with the concentration of *unbound* drug within the liver (this is, instantaneous and perfect distribution is assumed). Other models include *the parallel tube model* [3] and *the dispersion model* [6]. The parallel tube model assumes that the liver is composed of several identical, parallel tubes with enzymes distributed evenly in each cross section of the sinusoidal and perisinusoidal space. In this model, the hepatic unbound drug concentration declines within the organ along the direction of the blood flow. The dispersion model considers a nonideal flux within

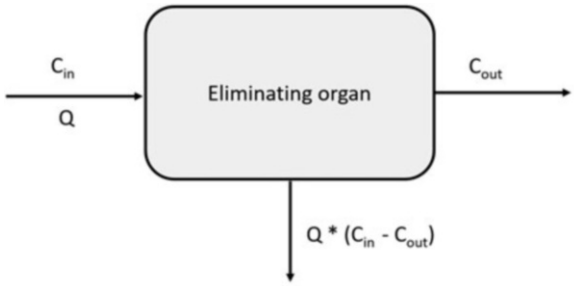

Total Clearance and Organ Clearance, Fig. 1 Schematic representation of the well-stirred model of hepatic clearance. The organ is perfused under steady-state conditions: C_{in} is the drug concentration in the blood entering the organ though the portal vein and the hepatic artery, whose contents are assumed to mix perfectly before partitioning into the sinusoids; C_{out} is the drug concentration in the blood leaving the organ through the hepatic vein; Q is the blood flow into the liver. In the context of the model, the drug distributes instantaneously and homogeneously within the single hepatic compartment

the organ, characterized by a dimensionless parameter called the dispersion number, which measures the spread in residence times of solute molecules moving through the liver, due to variations in velocity and path lengths covered by elements in the blood and by the branching and interconnection of sinusoids.

The assumptions of the well-stirred model are [3]:

a) Intimate mixing occurs between portal and arterial blood before the drug partitions into the sinusoids.
b) Only unbound drug can permeate through membranes and be subjected to elimination (see entry on ▶ "Free Drug Theory"). The rate of drug elimination is a function of the concentration of unbound drug within the organ.
c) No diffusional barrier exists between the blood and the enzymes within the hepatocytes; the distribution rate is thus entirely perfusion-limited. This is equivalent to saying that no drug concentration gradient exists within the liver. The unbound drug concentration is assumed to be uniform within the organ.

Based on a simple mass balance *at steady state*, where the drug distribution to the liver has been completed and the difference between the amounts of drug entering and exiting the organ are only due to the elimination processes, the rate of elimination of a drug by the organ is equal to the difference between the input and output rates of the drug through the organ:

$$\begin{aligned} &rate\ of\ elimination\ by\ the\ organ \\ &\quad = drug\ input\ rate - drug\ output\ rate \end{aligned} \tag{9}$$

The drug input rate to the organ can be expressed as the product of the blood flow Q and the drug concentration in the blood that enters the organ C_{in}. Comparably, the drug output rate can be written as the product of Q and the concentration in the blood that leaves the organ through the hepatic vein, C_{out} (note that, strictly speaking, the blood flux that enters the liver is not exactly equivalent to the blood flux that leaves the liver, the difference being the bile flow; nevertheless, this difference can be neglected as it corresponds to much less than 1% [3]). Accordingly:

$$rate\ of\ elimination = Q\ (C_{in} - C_{out}) \tag{10}$$

Following the definition of clearance, the hepatic clearance is the proportionality factor between the elimination rate by the organ and the input drug concentration. Therefore, by dividing both sides of Eq. (10) by C_{in}:

$$CL_H = \frac{Q\ (C_{in} - C_{out})}{C_{in}} \tag{11}$$

The ratio $(C_{in}\text{-}C_{out})/C_{in}$ is called the hepatic extraction ratio E_H, which represents the fraction

of the amount of drug entering the liver that is eliminated (extracted) by the organ. Therefore:

$$CL_H = Q \cdot E_H \tag{12}$$

The use of Eq. (12) requires the availability of blood (not plasma or serum) data. From such equation, it is evident that E_H can be estimated from the ratio between CL_H and Q. The use of plasma clearance, and liver blood flow for such purpose, or plasma clearance and liver plasma flow can result in substantial errors if R_b is different from 1. E_H is a dimensionless parameter ranging from 0 to 1, with $E_H = 0$ indicating that the organ does not eliminate the drug at all, while $E_H = 1$ indicates complete elimination of the drug entering the organ. Hepatic extraction represents the sum of extraction due to drug metabolism (E_{Hm}) plus extraction due to biliary excretion of unchanged drug (E_{Hb}). Depending on the value of E_H drugs are frequently classified as drugs with *high*, *intermediate*, or *low extraction ratio* [7, 8].

Drugs with $E_H > 0.7$ are classified as drugs with high extraction ratio. Examples of such drugs are propranolol, lidocaine, and morphine, among others. Here, the liver has such an intrinsic capacity to eliminate the drug that all the drug molecules in the blood are cleared as they pass through the liver, whether unbound or bound to plasma proteins or blood cells (this is known as nonrestrictive elimination). In this scenario, CL_H is perfusion-limited (i.e., it becomes sensitive to blood flow, as the liver can clear all the drug molecules that are presented to it, Fig. 2). These drugs typically have short elimination half-lives, and also a high first-pass hepatic effect when administered orally. At the other end of the spectrum are drugs with low extraction ratio

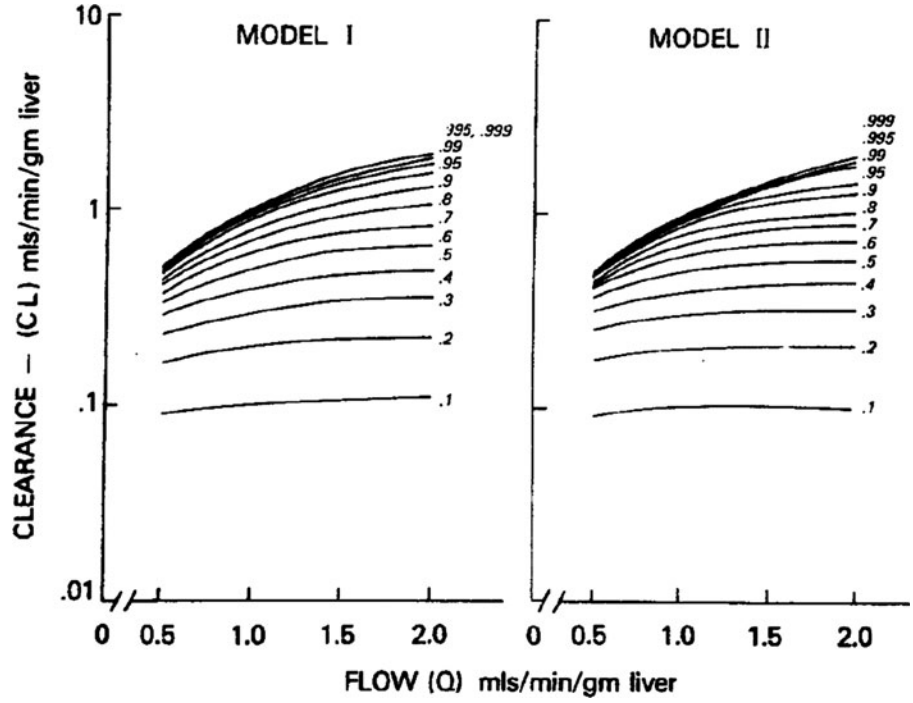

Total Clearance and Organ Clearance, Fig. 2 Relationship between hepatic clearance and the hepatic blood flow for drugs with different extraction ratios (extraction ratios are indicated next to each curve) for both the well-stirred (model I, on the left) and the parallel tube (model II, on the right) models. Note that the normal flow rate is about 1.0 ml/min/g liver. It can be appreciated that for high extraction ratio drugs, hepatic clearance increases (pseudo-linearly) with blood-flow above normal perfusion rate, thus being perfusion-limited. Contrariwise, for low extraction ratio drugs clearance practically does not change when blood flow increases. Reproduced from ref. [3] under permission of Springer Nature

($E_H < 0.3$) like warfarin, carbamazepine, and phenytoin. These are drugs for which hepatic clearance is capacity-limited (i.e., limited by the low intrinsic ability of the liver to eliminate them). Their metabolism will be essentially unchanged in low flow states, and clearance will be sensitive to changes in drug binding within the blood, as the elimination is restricted to unbound drug. For instance, warfarin clearance has been proven to be proportional to the fraction of unbound drug in plasma [9, 10]. These drugs typically present low first-pass hepatic metabolism after oral administration.

An important concept that deserves definition at this point is the intrinsic hepatic drug clearance CL_{int}, which reflects only the inherent ability of the organ to remove drug, in absence of restrictions imposed on drug delivery to the hepatocytes by neither protein binding nor blood flow [3, 11]. *Always in the context of the well-stirred model* (which assumes no diffusional barrier and instantaneous equilibration between the drug in the blood and the hepatocyte), CL_{int} relates the rate of hepatic elimination to the concentration of unbound drug surrounding the hepatic enzymes and the canalicular transporters [12–14], which will be denoted by $C_{L,u}$:

$$CL_{int} = \frac{rate\ of\ hepatic\ elimination}{C_{L,u}} \tag{13}$$

By definition, $CL_{int} > CL_H$ (as the former only considers unbound drug concentration in the liver that is always below or at most equal to the total drug concentration in blood or plasma). In fact, taking into consideration that if one assumes uniform concentrations between the blood and the liver, by combining Eqs. (11) and (13) the relationship between both parameters can be written as:

$$CL_H = CL_{int} \cdot f_u \tag{14}$$

f_u being the fraction of unbound drug in blood.

Note that often, within the specialized literature, the intrinsic clearance is exclusively related to drug elimination by metabolizing enzymes, probably due to historic reasons: at the time the parameter was introduced, nothing was still known on the role that efflux transporters play in the biliary secretion of the intact drug.

Hepatic drug elimination essentially depends on saturable processes (enzyme-mediated transformations, carrier-mediated efflux into the bile) that can be in general described by the Michaelis-Menten equation. If the intact drug is eliminated in the liver by n parallel processes (e.g., metabolism by different enzymes or metabolism plus secretion into the bile), the correspondent mass balance can be expressed as the sum of the rate of each parallel elimination process:

$$rate\ of\ hepatic\ elimination = \sum_{i=1}^{n} \frac{V_{max,i} C_{L,u}}{K_{M,i} + C_{L,u}} \tag{15}$$

where V_{max} denotes the maximum velocity achieved by each enzyme or efflux transporter, and K_M is the Michaelis-Menten constant. Then:

$$CL_H = \frac{1}{C_{in}} \sum_{i=1}^{n} \frac{V_{max,i} C_{L,u}}{K_{M,i} + C_{L,u}} \tag{16}$$

Also:

$$CL_{int} = \frac{1}{C_{L,u}} \sum_{i=1}^{n} \frac{V_{max,i} C_{L,u}}{K_{M,i} + C_{L,u}} = \sum_{i=1}^{n} \frac{V_{max,i}}{K_{M,i} + C_{L,u}} \tag{17}$$

Note that when $C_{L,u}$ is much lower than $K_{M,i}$ (meaning, far below saturating conditions), then the elimination process is apparently linear and CL_{int} reaches a constant maximum value $\sum_{i=1}^{n} \frac{V_{max,i}}{K_{M,i}}$.

Now, substituting expression (17) in expression (16):

$$CL_H = CL_{int} \frac{C_{L,u}}{C_{in}} \tag{18}$$

If we consider that $C_{L,u}$ equals $C_{out,u}$ (the unbound drug concentration in blood exiting the liver) [3]:

T

$$CL_H = CL_{int}\frac{C_{out,u}}{C_{in}} \quad (19)$$

$$CL_H = CL_{int}\frac{fu\ C_{out}}{C_{in}} \quad (20)$$

Considering Eq. (12), replacing C_{out}/C_{in} by $(1\text{-}E_H)$ and rearranging:

$$CL_H = Q\left[\frac{f_u CL_{int}}{f_u CL_{int} + Q}\right] \quad (21)$$

If Q can be neglected when compared with $f_u CL_{int}$, then Eq. (21) can be reduced to:

$$CL_H = Q \quad (22)$$

Hepatic clearance is flow-limited under these circumstances (non-restrictive elimination). Inversely, if $f_u CL_{int} \ll Q$, then:

$$CL_H = f_u CL_{int} \quad (23)$$

Hepatic clearance is restrictive in this case since it is limited by protein binding [14].

Renal clearance

The renal clearance of a drug, CL_R, includes the combination of glomerular filtration, tubular secretion, and tubular reabsorption, and also, for those drugs metabolized in the kidneys, renal biotransformation. Drug metabolism in the kidneys has sometimes been neglected when discussing renal clearance, as the contribution of these organs to drug metabolic clearance is usually less than that of liver (due to the lower microsome yield and organ weight of the kidneys). However, a considerable amount of data indicates that: a) the kidneys do have a substantial drug metabolizing capacity, and b) the activity of some drug-metabolizing enzymes in the kidney is comparable, or sometimes even higher than that in the liver [15, 16]. CL_R can be defined as the ratio between the rate of drug elimination by the kidneys and the drug concentration in the blood entering these organs through the renal arteries, which in this case corresponds to $C_{in.}$ In this respect, the rate of drug elimination in the kidneys can be calculated as:

$$\begin{aligned} &rate\ of\ renal\ drug\ elimination \\ &= V_{gf} + V_{ts} - V_{tr} + V_{m,k} \end{aligned} \quad (24)$$

where V_{gf} denotes the rate of glomerular filtration, V_{ts} represents the rate of tubular secretion, V_{tr} represents the rate of tubular reabsorption, and $V_{m,k}$ denotes the rate of drug metabolism in the kidneys (for more details on the physiologic aspects of renal excretion, the reader can refer to the entry on ▶ "Renal Drug Excretion"). Reasonably, the term that corresponds to the rate of the reabsorption is negative, as reabsorption restricts drug elimination.

Analogously to what is seen in the section of hepatic clearance (Eq. 12), the renal extraction ratio E_r can be defined as:

$$E_r = \frac{CL_R}{Q} \quad (25)$$

where Q is, in this case, the blood flow into the kidneys. The drugs can be classified according to their extraction ratios, similarly to what was previously discussed for hepatic extraction. Compounds with low renal extraction ratios include gentamycin, lithium, tetracyclines, and digoxin, among many others. Penicillins constitute a classic example of compounds with high renal extraction [17], with a predominant role of active tubular secretion in their renal elimination.

Glomerular filtration markers are usually used in the clinical laboratory to assess the glomerular filtration rate (GFR) of an individual. An ideal marker of the filtration rate must gather the following characteristics [18]: a) its only route of elimination must be through the kidney via glomerular filtration; b) it should not subject to plasma protein binding; c) it should not be subject to tubular secretion or reabsorption. Inulin is usually referred as the gold standard marker of glomerular filtration. Creatinine is however the most extensively used marker of glomerular filtration, despite it is subject to some tubular secretion and reabsorption. The GFR is about 75–115 mL per minute for women and 85–125 mL per minute for men [19]. If we take into consideration that renal blood flow is between 1.0 and 1.2 L per minute per 1.73 m^2 of body surface area, it becomes

evident that drugs extracted only by glomerular filtration will present very low extraction ratios, and even less if the drug is subject to tubular reabsorption. Therefore, they will be restrictively eliminated: only unbound drug molecules will be filtered through the glomerulus. Consider then that the clearance due to glomerular filtration will match the GFR only if the cleared substance is not bound to plasma proteins or other blood elements; otherwise, the GFR should be multiplied by f_u.

In contrast, compounds with high extraction ratios in the kidneys can be nonrestrictively removed, that is, protein-bound drug molecules can be removed from the protein-drug complex during a single passage through the kidney.

When the drug is subject to tubular secretion by efflux proteins located in the luminal membrane of the tubular epithelium and/or to metabolism by tubular enzymes, by analogy with Eq. (21), an assuming no tubular reabsorption, CL_R can be expressed as:

$$CL_R = f_u \left(GFR + Q \left[\frac{CL_{int}}{CL_{int} + Q} \right] \right) \quad (26)$$

Now, to account for tubular reabsorption, Eq. (26) may be corrected resorting to the fraction of filtered and secreted drug that is reabsorbed, F_r:

$$CL_R = f_u \left(GFR + Q \left[\frac{CL_{int}}{CL_{int} + Q} \right] \right) \times (1 - F_r) \quad (27)$$

As seen in the preceding section for other organs, the total pulmonary clearance CL_P would involve the drug extraction due to metabolizing enzymes expressed in the lung plus drug excretion though the expelled air, which could contribute to pulmonary clearance in the case of volatile drugs. The expression of drug metabolizing enzymes in lungs is known to be much lower than that of the liver (for instance, it has been estimated that CYP450 drug metabolism represents less than 10% of that found in the liver), and the contribution of the lungs to the total body mass is rather small [20, 21]; therefore, pulmonary clearance is not considered, in general, as a significant contributor to systemic clearance.

The lungs can however affect the blood concentrations of drugs administered intravenously (first-pass pulmonary effect) because of their strategic location between the site of administration and the site of action and their high perfusion, which enables the rapid partitioning of drugs [21]. Some particular enzymes expressed in the lungs, namely esterases, can also be exploited pharmacologically for the design of inhaled prodrugs [22, 23].

Estimation of Organ Clearances

Direct estimation of organ clearances can be performed by taking advantage of a generalization of Eq. (12):

$$CL_O = Q \cdot E_O \quad (28)$$

where CL_O represents the clearance of the organ of interest, Q the blood flow into that organ, and E_O denotes the extraction ratio of the drug by that organ. By directly measuring the extraction ratio, and knowing the organ blood flow, it is possible to estimate the organ clearance. Nevertheless, direct estimation of the extraction ratio requires invasive surgical procedures to insert catheters in multiple blood vessels, and also laparotomy, or, alternatively, isolated organ perfusion techniques [24, 25]. These approximations are predominantly feasible when studying drug elimination in animal models.

If the drug is completely eliminated by the liver, CL_O can be readily estimated from the blood concentration-time data after intravenous administration of the drug using Eq. (4), as in that case systemic clearance and hepatic clearance will be identical. If the drug is cleared by both the liver and the kidneys (and no other organ), and if CL_R can be measured, CL_H can be indirectly estimated by subtracting CL_R from the overall (systemic) clearance. This approach can be used both in animal and human studies.

Regarding estimation of CL_R, one possibility involves resorting to a derivation of Eq. (1):

$$CL_R = \frac{\frac{dA_{e,R}}{dt}}{C_p} \tag{29}$$

where $A_{e,R}$ denotes the amount of drug that has been eliminated by the kidneys. As the instantaneous rate of elimination $\frac{dA_{e,R}}{dt}$ cannot be easily measured, Eq. (29) is adapted to non-infinitesimal increments:

$$CL_R = \frac{\frac{\Delta A_{e,R}}{\Delta t}}{C_{p,mid}} \tag{30}$$

Now, urine is collected at time intervals Δt, and the amount of drug in each urine sample analytically determined. $C_{p,mid}$ denotes the plasma concentration at the mid-point of the urine collection interval. If CL_R is independent of the drug concentration, a plot of $\frac{\Delta A_{e,R}}{\Delta t}$ versus $C_{p,mid}$ should provide a straight line with slope CL_R. It is suggested to use short collection intervals, when possible. Ideally, $C_{p,mid}$ should be measured in arterial blood: if peripheral venous samples are used, their early drug content may be considerable lower than that in the renal arteries. Another source of error relates to the fact that the rate of urinary excretion lags behind the plasma drug concentration in about 5 minutes, due to the flow or urine through the dead space of the kidneys and the ureters [26]. When tubular secretion represents a significant fraction of the CL_R, disequilibrium between plasma concentrations and the highly dynamic concentrations in the interstice around the peritubular vascular space will also cause deviations.

Expression (30) is often presented as:

$$CL_R = \frac{Q_u\, C_u}{C_{p,mid}} \tag{31}$$

where Q_u is urine flow rate and C_u denotes the concentration of drug in urine.

Mathematical issues with the choice of Δt are avoided if the renal clearance is estimated during steady state, administering the drug through continuous intravenous infusion.

A second method to estimate CL_R is based on expressing Eq. (29) as:

$$CL_R = \frac{dA_{e,R}}{dt\, C_p} \tag{32}$$

By integrating the numerator and the denominator from time zero to infinity:

$$CL_R = \frac{A_{e,R\ 0-\infty}}{AUC_{0-\infty}} \tag{33}$$

Here, $A_{e,R\ 0\text{-}\infty}$ is the total amount of unchanged drug recovered in urine (Eqs. 29–32 assume that no biotransformation of the drug occurs in the kidney, or refers only to renal clearance due to unchanged drug excretion). This second method is insensitive to uncertainties in the time of urine collection, in contrast to the formerly discussed one.

Cross-References

- ▶ Biliary Drug Excretion
- ▶ Drug Excretion
- ▶ Noncompartmental Pharmacokinetics
- ▶ One-Compartment Pharmacokinetic Model
- ▶ Physiologically Based Pharmacokinetic Modeling: Definition and History
- ▶ Renal Drug Excretion
- ▶ Two-Compartment Pharmacokinetic Model

References

1. Toutain PL, Bousquet-Mélou A. Plasma clearance. J Vet Pharmacol Ther. 2004;27(6):415–25.
2. Horde GW, Gupta V. Drug clearance. [Updated 2020 Oct 11]. In: StatPearls [Internet]. Treasure Island: StatPearls Publishing; 2020. Available from: https://www.ncbi.nlm.nih.gov/books/NBK557758/.
3. Pang KS, Rowland M. Hepatic clearance of drugs. I. Theoretical considerations of a "well-stirred" model and a "parallel tube" model. Influence of hepatic blood flow, plasma and blood cell binding, and the hepatocellular enzymatic activity on hepatic drug clearance. J Pharmacokinet Biopharm. 1977;5:625–53.

4. Smith DA, Beaumont K, Maurer TS, Di L. Clearance in drug design. J Med Chem. 2019;62:2245–55.
5. Uchimura T, Kato M, Saito T, Kinoshita H. Prediction of human blood-to-plasma drug concentration ratio. Biopharm Drug Dispos. 2010;31:286–97.
6. Roberts MS, Rowland M. Correlation between in-vitro microsomal enzyme activity and whole organ hepatic elimination kinetics: analysis with a dispersion model. J Pharm Pharmacol. 1986;38:177–81.
7. Lammers LA, Achterbergh R, Romijn JA, Mathôt RAA. Short-term fasting alters pharmacokinetics of cytochrome P450 probe drugs: does protein binding play a role? Eur J Drug Metab Pharmacokinet. 2018;43:251–7.
8. Herbert MF. Impact of pregnancy on maternal pharmacokinetics of medications. In: Mattison DR, editor. Clinical pharmacology during pregnancy. Cambridge: Academic Press; 2013. p. 17–39.
9. Yacobi A, Udall JA, Levy G. Serum protein binding as a determinant of warfarin body clearance and anticoagulant effect. Clin Pharmacol Ther. 1976;19:552–8.
10. Routledge PA, Chapman PH, Davies DM, Rawlins MD. Pharmacokinetics and pharmacodynamics of warfarin at steady state. Br J Clin Pharmacol. 1979;8:243–7.
11. Wilkinson GR, Shand DG. Commentary: a physiological approach to hepatic drug clearance. Clin Pharmacol Ther. 1975;18:377–90.
12. Verbeeck RK. Pharmacokinetics and dosage adjustment in patients with hepatic dysfunction. Eur J Clin Pharmacol. 2008;64:1147–61.
13. Kusuhara H, Sugiyama Y. In vitro-in vivo extrapolation of transporter-mediated clearance in the liver and kidney. Drug Metab Pharmacokinet. 2009;24:37–52.
14. Susla GM, Lertora JJL. Effect of liver disease on pharmacokinetics. In: Atkinson AJ, Huang SM, Lertora JJL, Markey SP, editors. Principles of clinical pharmacology. Cambridge: Academic Press; 2012. p. 81–96.
15. Knights KM, Rowland A, Miners JO. Renal drug metabolism in humans: the potential for drug-endobiotic interactions involving cytochrome P450 (CYP) and UDP-glucuronosyltransferase (UGT). Br J Clin Pharmacol. 2013;76:587–602.
16. Gibson TP. Renal disease and drug metabolism: an overview. Am J Kidney Dis. 1986;8:7–17.
17. Eagle H, Newman E. The renal clearance of penicillins F, G, K, and X in rabbits and man. J Clin Invest. 1947;26:903–18.
18. Seegmiller JC, Eckfeldt JH, Lieske JC. Challenges in measuring glomerular filtration rate: a clinical laboratory perspective. Adv Chronic Kidney Dis. 2018;25:84–92.
19. Britannica. The editors of encyclopedia. Inulin clearance. Encyclopedia Britannica, 7 Feb 2019. https://www.britannica.com/science/inulin-clearance. Accessed 11 Feb 2021.
20. Somers GI, Lindsay N, Lowdon BM, Jones AE, Freathy C, Ho S, et al. A comparison of the expression and metabolizing activities of phase I and II enzymes in freshly isolated human lung parenchymal cells and cryopreserved human hepatocytes. Drug Metab Dispos. 2007;35:1797–805.
21. Liu X, Jin L, Upham JW, Roberts MS. The development of models for the evaluation of pulmonary drug disposition. Expert Opin Drug Metab Toxicol. 2013;9:487–505.
22. Nave R. Determination of lung deposition following inhalation of ciclesonide using different bioanalytical procedures. Bioanalysis. 2010;2:807–14.
23. Gabriele M, Puccini P, Lucchi M, Vizziello A, Gervasi PG, Longo V. Presence and inter-individual variability of carboxylesterases (CES1 and CES2) in human lung. Biochem Pharmacol. 2018;150:64–71.
24. Mehvar R. Application of organ clearance to estimation of the in vivo hepatic extraction ratio. Curr Clin Pharmacol. 2016;11:47–52.
25. Liu Y, Weber SJ, Onua ET. Hepatic clearance and drug metabolism using isolated perfused rat liver. Curr Protoc Pharmacol. 2004; Chapter 7: Unit 7.9.
26. Tucker GT. Measurement of the renal clearance of drugs. Br J Clin Pharmacol. 1981;12:761–70.

Traffic ATPases

► ABC Transporters: An Overview

Transcytosis in Drug Absorption and Distribution

Alan Talevi[1,2] and Carolina L. Bellera[1,3]
[1]Laboratory of Bioactive Research and Development (LIDeB), Department of Biological Sciences, University of La Plata (UNLP), La Plata, Buenos Aires, Argentina
[2]Argentinean National Council of Scientific and Technical Research (CONICET) – CCT, La Plata, Buenos Aires, Argentina
[3]Consejo Nacional de Investigaciones Científicas y Técnicas (CONICET), La Plata, Buenos Aires, Argentina

Synonyms

Endocytosis, Exocytosis

Definition

The term transcytosis designates the vesicular transcellular transport of molecules from one side of a polarized epithelial or endothelial cell to the other. It is a key process for the absorption and/or distribution of large molecules, e.g., macromolecules, or, in some cases, more complex entities, e.g., nanoscale particles/constructs.

Vesicular Transference Across Epithelia and Endothelia

Epithelial cell layers line the outer surfaces of organs throughout the body, as well as the inner surfaces of cavities in many internal organs. They act as selective barriers, regulating the transference of molecules (and, at times, supramolecular structures) in and out of organs. Endothelial cell layers, which line the interior surface of the blood vessels, accomplish an equivalent function in separating the vascular space from the extravascular tissues. They are thus critical barriers in the processes of drug absorption and distribution for systemic drug delivery. Drug molecules or, occasionally, drug delivery systems must overcome them to reach the bloodstream, in the first place, and then the site of action, so that they can exert their pharmacological effect. Relevant epithelia for drug absorption are found, for instance, in the mucosa of the gastrointestinal tract (for buccal, sublingual, oral, and rectal delivery) and the respiratory tract (for pulmonary delivery). Tight junctions link adjacent epithelial cells. These junctions regulate the diffusive movement of solutes across the cell layer (by the paracellular pathway), and they also divide the plasma membrane of each cell into apical and basolateral domains, each one containing a unique set of membrane proteins and lipids (polarized cells). The apical plasma membrane faces the luminal space, while the basolateral one faces the blood supply. Endothelial barriers are organized in a similar manner, except that the apical membrane faces the vascular space, and the basolateral membrane faces the extravascular tissues. Such polarized configuration allows the vectorial transport of substances across the cell layer.

Understanding transcytosis is particularly relevant for the bioavailability of certain therapeutic agents in the brain, as the transcellular and paracellular pathways are greatly diminished there by the presence of blood-brain barrier, as discussed later [1, 2].

The term transcytosis refers to the transport of molecular or supramolecular structures from one side of an epithelial or endothelial cell to the other, through membrane trafficking (i.e., vesicular transport) [3]. Despite this entry focuses on drug delivery and potential clinical applications of transcytosis, it is worth noting that this mechanism is also relevant in infectious processes (see [4, 5]) and for the transference of physiological elements [6].

To begin with, transcytosis first requires cellular uptake through *endocytosis* (that is, an energy-driven process in which the cargo is internalized surrounded by an area of the cell membrane, which buds off inside the cell to form a vesicle). At present, the term endocytosis is used to denote all kinds of cellular ingestion. The classification of endocytic processes may vary depending on the author consulted. Usually, endocytosis is segregated in phagocytosis and pinocytosis. Phagocytosis involves the recognition and ingestion of relatively large particles (in the submicrometric range and above, e.g., pathogenic microorganisms, foreign material, and tissue debris); in higher organisms, it is a key process of immune and inflammatory responses, being undertaken by specialized ("professional") cells (phagocytes) [7]. Further attention will not be given to phagocytosis within this entry, although it may impact the response to some therapeutic systems (e.g., it plays a key role in the fast clearance of nanosystems from the bloodstream, and it may be exploited for targeted drug delivery systems in cancer and inflammatory disorders [8, 9]).

Pinocytosis ("cell sipping" or "cell drinking"), on the other hand, refers to a process by which the cell takes in pericellular fluid along with dissolved small molecules and can be undertaken by most cell types. Broadly speaking, pinocytosis can be described as macro- and micropinocytosis, and

the latter, in turn, can be classified as clathrin-dependent, caveolae-dependent, and clathrin/caveolae-independent endocytosis [10]. This classification is based on the proteins (clathrin and caveolin) involved in the endocytic process, and thus it may overlap with other classifications based on different criteria, like receptor-mediated or adsorptive-mediated endocytosis (see next section).

Macropinocytosis results in relatively large vesicles with sizes approximately ranging from 0.2 to 10μm in diameter [11]. The remaining types of pinocytosis can be collectively referred as microscale endocytic phenomena (micropinocytosis), as the sizes of the vesicles formed are below 200 nm. Depending on the type of endocytosis, it may be triggered by more or less specific stimuli, an aspect that will also determine the saturability of the process. Receptor-mediated endocytosis is the most specific type (i.e., a comparatively high affinity but low-capacity process). It generally occurs via the clathrin-dependent pathway [10], and it is currently suspected that many events previously thought as nonspecific pinocytosis are in fact due to receptor-mediated endocytosis. In the clathrin-dependent pathway (the most studied endocytic pathway), binding of a ligand to a surface receptor induces the polymerization of clathrin, a protein that aggregates in a polyhedral lattice that facilitates changes in membrane curvature, ultimately surrounding the ligand and forming the vesicle [12]. Once the vesicle is separated from the cell surface, the coat is rapidly dropped and recycled for further endocytic events.

After endocytosis, the internalized cargo navigates through intracellular, membrane-enclosed compartments until occasionally reaching the opposite plasma membrane is reached, when vesicle fusion occurs, and the cargo is released to the pericellular space.

Classification of Transcytosis

Transcytosis may be classified in different manners: *direct* versus *indirect*, and *unspecific* versus *receptor-mediated*.

In the case of **direct transcytosis**, the vesicle, once formed after endocytosis, is transported unchanged to the opposite side, where it fuses with the plasma membrane (Fig. 1). In other words, a unique vesicle acts as a shuttle between the apical and basal surfaces. Caveolae-mediated

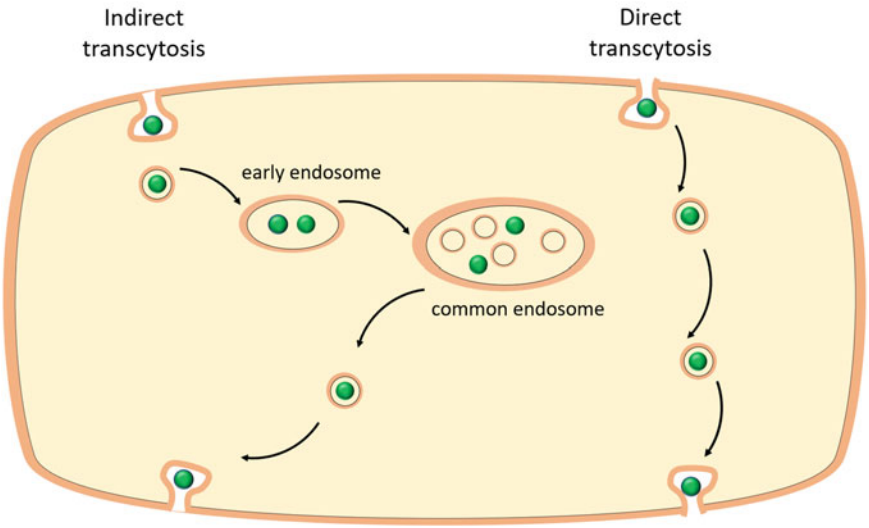

Transcytosis in Drug Absorption and Distribution, Fig. 1 Schematic representation of the direct and indirect transcytosis mechanisms

transport in endothelia seems to be the most common route of direct transcytosis [6, 13].

On the other hand, the endosomal system plays a fundamental role in **indirect transcytosis** (Fig. 1). Formed by a collection of diverse, dynamic vesicles, including early sorting endosomes and late endosomes/lysosomes, and extending to the vesicular trans-Golgi network and phagosomes, the endosomal system includes a comparatively immobile perinuclear pool and a much more dynamic group of vesicles occupying the cell periphery [14]. Once taken up from the pericellular space, early endosomes move toward the perinuclear population, to mature into the late proteolytic compartments. At present, neither the apical nor basolateral early endosomes are thought to deliver their cargo directly to the contralateral plasma membrane [15]. The endoplasmic reticulum seems to exert a crucial role in monitoring the intracellular coordinates of the endosomal system constituents [14]. In indirect transcytosis, the cargo first localizes in early endosomes, and it is therefore transferred to other vesicular compartments that eventually pass the cargo to vesicles specialized for exocytosis on the opposite side of the cell [3]. Newly formed endocytic vesicles fuse to constitute the sorting endosome (alternatively, they may fuse with preexisting sorting endosomes), where the fate of their cargo is defined [16]. The absorption of plasma membrane elements is compensated by the return of membrane cargo to the surface through endosomal recycling. This strategy contributes to maintaining the homeostatic and differential composition of the apical and basolateral membranes of polarized cells. The compartments shared by the apical and basolateral sorting endosomes include the late endosome and lysosome, the endoplasmic reticulum, the Golgi network, and the common recycling endosome (a stable structure located in the apical perinuclear region of the cell). The latter is thought to receive cargo from both luminal early sorting endosomes and sorts them back to the cell surface where endocytosis took place, for recycling, or to the opposite one, for transcytosis [15].

Unspecific transcytosis comprises *adsorptive-mediated transcytosis* and *fluid phase transcytosis*.

In *adsorptive-mediated transcytosis*, the cell membrane invagination is triggered by an electrostatic interaction between cationic molecules (typically, a short amino acid sequence that features hydrophobic residues and residues that are positively charged under physiological conditions) and anionic microdomains on the cell membrane [17]. This phenomenon may be therapeutically exploited through the use of polycationic cell-penetrating peptides (CPPs) that can drive the uptake of a variety of molecular entities and constructs, from nanodevices to DNA. This said, it must be noted that the endocytic mechanism used by CPPs seems to depend on the CPP nature, and that for some CPPs multiple endocytic pathways might be simultaneously used [17–19]. CPPs also appear to promote the escape from endocytic vesicles, an essential step for intracellular delivery, possibly by disrupting the endosomal membrane. Moreover, the escape from endosomes might be enhanced through the incorporation of fusogenic lipids, membrane-disruptive peptides, and endosomolytic agents to the delivery systems [19].

In *fluid phase transcytosis* (also known as bulky-phase transcytosis), soluble plasma molecules are randomly uptaken by caveolae with a bulk of extracellular fluid, and then transferred. The process is independent of any interaction between the vesicle membrane and the transported molecules; remarkably, the frequency of caveolae varies considerably across tissues [3, 17].

Receptor-mediated transcytosis, in contrast, is triggered by specific receptor recognition events that induce endosome formation. Well-known examples of this type of transcytosis include transferrin, insulin, and low-density lipoprotein (LDL) transcytosis [17, 20], among others (see Figs. 2 and 3, illustrating the transcytosis pathway of LDL and immunoglobulin A).

Clinical Applications and Limitations

Transcytosis might be clinically exploited for the delivery of therapeutic molecules which, due to their physicochemical features (e.g., size), would hardly reach their target otherwise. As examples, we can cite therapeutic peptides and proteins (for

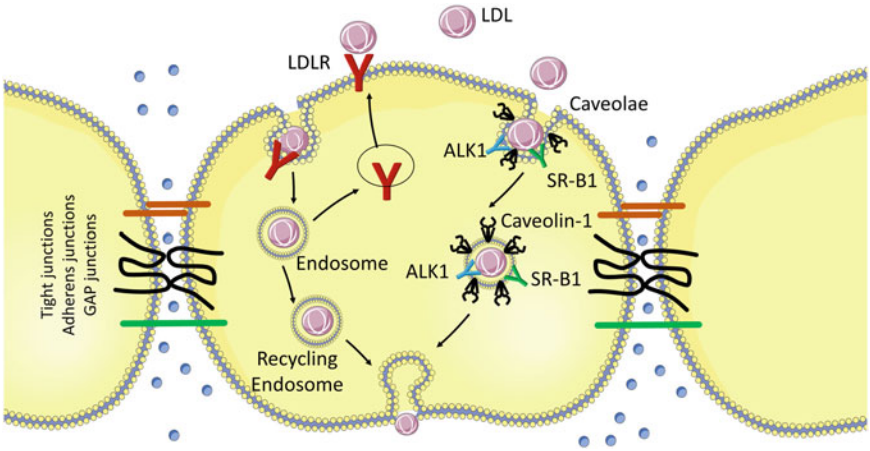

Transcytosis in Drug Absorption and Distribution, Fig. 2 Schematic representation of low-density lipoprotein (LDL) transcytosis by endothelial cells. Water and small molecules are transported across endothelial cells by the paracellular route. The classical LDL receptor (LDLR) pathway mediates LDL uptake and its degradation in the lysosomes, which is not essential for transcytosis. LDL can transpose endothelial cells through receptor-mediated transcytosis associated with scavenger receptor B1 (SR-B1), activin receptor-like kinase 1 (ALK1), or LDL receptor (LDLR), as well as caveolae-mediated direct transcytosis. The endocytosed LDL particles are then transferred to the opposite side of the cell directly (caveolae-mediated transcytosis) or indirectly (receptor-mediated transcytosis) and exocytosed to the subendothelial space

instance, antibody-based therapeutics), as well as other large molecules (for instance, oligonucleotide-based gene editing) [15] (see entries ▶ "Absorption of Biotechnology-Derived Biologics Drug Products" and ▶ "Distribution of Biotechnology-Derived Biologics Drug Products"). The transport of large biologics across mucosal and endothelial barriers is one of the main hurdles for biopharmaceuticals development, limiting their oral bioavailability and their biodistribution to some specific body compartments (e.g., the brain). Another obstacle that usually impairs drug delivery of biopharmaceuticals is the lack of stability in the biological environment (e.g., acidic gastric environment, exposure to degradative enzymes, etc.).

Endocytosis and transcytosis also play a central role in the delivery of therapeutic agents encapsulated or adsorbed by pharmaceutical nanocarriers and other last generation drug delivery vectors such as viral vectors [20, 21]. Such emerging pharmaceutical carriers could be useful for the delivery of both biotherapeutics and small molecules with an unfavorable biopharmaceutical profile (poor solubility and/or permeability, limited in vivo stability). Furthermore, off-target safety issues might be circumvented or attenuated using targeted drug delivery vectors. In any case, one limiting step in achieving an effective delivery of therapeutics across epithelia and/or endothelia is the prevention of lysosomal sorting, which otherwise leads to early/off-target degradation of the drug delivery vector and/or its therapeutic cargo [17, 22, 23].

Potentially, all the transcytosis pathways described in the previous section may be exploited for the delivery of therapeutics, each one with its correspondent advantages and disadvantages [17]. For instance, CPPs have been extensively studied to facilitate cell uptake of biotherapeutics and nanocarriers. Among their pros, it may be mentioned that their uptake is saturated at much higher concentrations than in receptor-mediated endocytosis/transcytosis, that they are also less likely to interfere with cell-signaling pathways, and that their transport is less dependent on specific recognition events. Among their limitations, we can list their rather unspecific biodistribution, their potential to bind to serum proteins (which may increase their circulating time but also negatively impact on their distribution), and the fact that their toxicity and immunogenicity is still poorly understood, thus deserving more focus in future studies [23, 24]. On the other hand, whereas

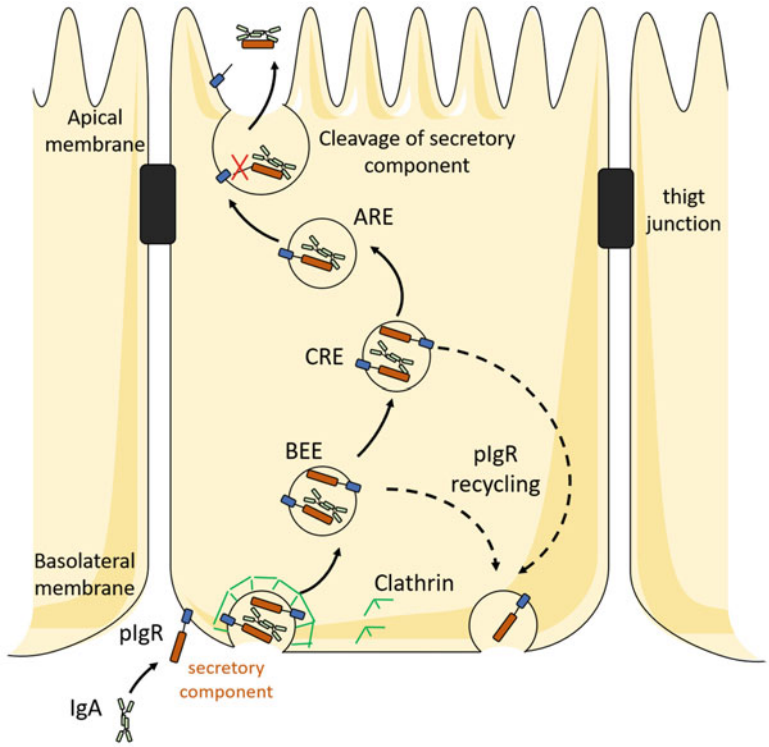

Transcytosis in Drug Absorption and Distribution, Fig. 3 Schematic representation of *polymeric immunoglobulin receptor* (pIgR)-mediated immunoglobulin A transcytosis. At the basolateral plasma membrane, the pIgR is internalized by clathrin-coated pits into basolateral early endosomes (BEE). This happens without binding of immunoglobulin A (IgA) to pIgR. Without bound IgA, pIgR is preferentially recycled to the basolateral plasma membrane but can also continue to the apical plasma membrane (transcytotic route). With bound IgA, transcytosis of pIgR is enhanced. The IgA-pIgR complex continues to common recycling endosomes (CRE) and apical recycling endosomes (ARE) before it reaches the apical plasma membrane. The release of IgA requires cleavage of the secretory component of pIgR

receptor-mediated transcytosis opens the possibility of a much more specific drug delivery, limited capacity might be observed due to the limited receptor expression levels. Hence, competition with physiologic substrates may raise safety issues and variable absorption and distribution kinetics. Also, lysosomal sorting may occur preventing exocytosis of the cargo [17].

Transcytosis-mediated drug absorption and distribution is a critical point to fully exploit many last generation therapeutic technologies, from biopharmaceuticals to nanodelivery systems (see the entry ▶ "Pharmaceutical Nanocarriers: Absorption" and ▶ "Active Targeting of Nanocarriers" for further details). Enhanced absorption of otherwise nonbioavailable drugs and selective distribution by active targeting are relevant but so far much unfulfilled ideas, at least at the clinical level. The numerous attempts to understand and exploit the phenomenon have greatly advanced the knowledge on transepithelial and transendothelial drug delivery and how delivery vectors may be tailored to avoid lysosomal sorting if necessary, thus completing a successful transcytosis event.

Cross-References

- ▶ Absorption of Biotechnology-Derived Biologics Drug Products
- ▶ Active Targeting of Nanocarriers

▶ Distribution of Biotechnology-Derived Biologics Drug Products
▶ Pharmaceutical Nanocarriers: Absorption.

References

1. Gao X, Gu X, Chen H. The distribution and elimination of nanomaterials in brain. In: Jiang X, Gao H, editors. Neurotoxicity of nanomaterials and nanomedicine. Burlington: Academic; 2017. p. 59–74.
2. Preston JE, Joan Abbott N, Begley DJ. Transcytosis of macromolecules at the blood-brain barrier. Adv Pharmacol. 2014;71:147–63.
3. Thuenauer R, Müller SK, Römer W. Pathways of protein and lipid receptor-mediated transcytosis in drug delivery. Expert Opin Drug Deliv. 2017;14(3):341–51.
4. Bomsel M. Transcytosis of infectious human immunodeficiency virus across a tight human epithelial cell line barrier. Nat Med. 1997;3(1):42–7.
5. Tugizov SM, Herrera R, Palefsky JM. Epstein-Barr virus transcytosis through polarized oral epithelial cells. J Virol. 2013;87(14):8179–94.
6. Tuma P, Hubbard AL. Transcytosis: crossing cellular barriers. Physiol Rev. 2003;83(3):871–932.
7. Rosales C, Uribe-Querol E. Phagocytosis: a fundamental process in immunity. Biomed Res Int. 2017;2017:9042851.
8. Gustafson HH, Holt-Casper D, Grainger DW, Ghandehari H. Nanoparticle uptake: the phagocyte problem. Nano Today. 2015;10:487–510.
9. Hu G, Guo M, Xu J, Wu F, Fan J, Huang Q, et al. Nanoparticles targeting macrophages as potential clinical therapeutic agents against cancer and inflammation. Front Immunol. 2019;10:1998.
10. Xu Y, Xia J, Liu S, Stein S, Ramon C, Xi H, et al. Endocytosis and membrane receptor internalization: implication of F-BAR protein Carom. Front Biosci (Landmark Ed). 2017;22:1439–57.
11. Kumari S, Mg S, Mayor S. Endocytosis unplugged: multiple ways to enter the cell. Cell Res. 2010;20(3):256–75.
12. Donaldson JG. Endocytosis. In: Lennarz WJ, Lane MD, editors. Encyclopedia of biological chemistry. Amsterdam: Academic; 2013. p. 197–9.
13. Zhang X, Sessa WC, Fernández-Hernando C. Endothelial transcytosis of lipoproteins in atherosclerosis. Front Cardiovasc Med. 2018;5:130.
14. Neefjes J, Jongsma MML, Berlin I. Stop or go? Endosome positioning in the establishment of compartment architecture, dynamics, and function. Trends Cell Biol. 2017;27(8):580–94.
15. Garcia-Castillo MD, Chinnapen DJ, Lencer WI. Membrane transport across polarized epithelia. Cold Spring Harb Perspect Biol. 2017;9(9):a027912.
16. Li X, DiFiglia M. The recycling endosome and its role in neurological disorders. Prog Neurobiol. 2012;97(2):127–41.
17. Abdul Razzak R, Florence GJ, Gunn-Moore FJ. Approaches to CNS drug delivery with a focus on transporter-mediated transcytosis. Int J Mol Sci. 2019;20(12):3108.
18. Kalafatovic D, Giralt E. Cell-penetrating peptides: design strategies beyond primary structure and amphipathicity. Molecules. 2017;22(11):1929.
19. Ruseska I, Zimmer A. Internalization mechanisms of cell-penetrating peptides. Beilstein J Nanotechnol. 2020;11:101–23.
20. Jones AR, Shusta EV. Blood-brain barrier transport of therapeutics via receptor-mediation. Pharm Res. 2007;24(9):1759–71.
21. Stanimirovic DB, Sandhu JK, Costain WJ. Emerging technologies for delivery of biotherapeutics and gene therapy across the blood-brain barrier. BioDrugs. 2018;32(6):547–59.
22. Rathore B, Sunwoo K, Jangili P, Kim J, Kim H, Huang M, et al. Nanomaterial designing strategies related to cell lysosome and their biomedical applications: a review. Biomaterials. 2019;211:25–47.
23. Hervé F, Ghinea N, Scherrmann JM. CNS delivery via adsorptive transcytosis. AAPS J. 2008;10(3):455–72.
24. Skotland T, Iversen TG, Torgersen ML, Sandvig K. Cell-penetrating peptides: possibilities and challenges for drug delivery in vitro and in vivo. Molecules. 2015;20(7):13313–23.

Transdermal Drug Delivery

Marcelo Carlos Nacucchio[1] and Héctor Juan Prado[2,3]
[1]Departamento de Tecnología Farmacéutica, Cátedra de Tecnología Farmacéutica II, Universidad de Buenos Aires, Facultad de Farmacia y Bioquímica, Buenos Aires, Argentina
[2]Cátedra de Tecnología Farmacéutica II, Departamento de Tecnología Farmacéutica, Facultad de Farmacia y Bioquímica, Universidad de Buenos Aires, Buenos Aires, Argentina
[3]Instituto de Tecnología de Alimentos y Procesos Químicos (ITAPROQ), CONICET - Universidad de Buenos Aires, Buenos Aires, Argentina

Synonyms

Emplastra transcutanea; Self-adhering transdermal drug delivery systems (TDS); Transdermal patches

Definition

The European Pharmacopoeia and the United States Pharmacopeia share similar definitions of transdermal delivery systems (TDS) which are presented as follows, respectively:

- TDS are flexible pharmaceutical preparations of varying sizes, containing one or more active substances. They are intended to be applied to the unbroken skin in order to deliver the active substance(s) to the systemic circulation after passing through the skin barrier [1].
- TDS are placed onto intact skin to deliver the drug to the systemic circulation. They are designed for prolonged release (up to 7 days) [2].

Historical Development

Topical remedies applied to the skin have been used since the origin of man, in most ancient cultures. References of medicated plasters (emplastra) can be found in ancient China (around 2000 BC). These early plasters generally contained multiple ingredients of herbal drugs dispersed into an adhesive natural gum rubber base, applied to a backing support made of fabric or paper. The concept that certain drugs cross the skin appears to have been applied by Ibn Sina (or Avicenna, AD 980–1037), a Persian physician who used many emplastra for topical or systemic treatments. Mercurial ointments, for example, were used in the fifteenth century for the treatment of syphilis. During the last decades of the nineteenth century, there was a stage of disbelief in the systemic effects of emplastra formulations. Those ideas reversed along the twentieth century, when significative scientific evidence accumulated in relation to the percutaneous absorption of drugs [3].

In 1979, a circular filmlike 1.5 cm in diameter patch, programmed to deliver 0.5 mg of scopolamine over 3 days, was the first transdermal patch to reach the US market [4]. In the following decade, transdermal patches of nicotine became the first commercial success of a transdermal system, increasing the acceptance of transdermal administration in patients and in the medical community. In the last decades, there has been a continuous increase in the number of patches approved by the regulatory authorities. Currently, there are various transdermal delivery systems for drugs such as estradiol, fentanyl, lidocaine, testosterone, combination patches with more than one drug for contraception or hormonal replacement, and iontophoretic or ultrasonic administration systems for analgesia [5].

The global transdermal skin patches market has grown constantly along the twenty-first century and was worth 6.23 billion US dollars in 2019. It is expected to grow at a compound annual growth rate of 4.5% until 2023 [6].

Advantages and Challenges

Transdermal delivery presents advantages when compared with the oral and parenteral routes. Transdermal route avoids liver first-pass effect that reduces the oral bioavailability of some drugs. It also avoids the pain, dangerous medical waste generation, and the risk of disease transmission associated with hypodermic injections. As a result of their external localization, transdermal systems are noninvasive and can be easily self-administered and controlled by the patient [7]. Also, these systems can provide drug release for long periods of time (up to 1 week), improving patient compliance, and they are generally inexpensive [8, 9]. One of the greatest challenges for transdermal delivery is that only a limited number of drugs can be directly administered by this route with conventional systems, due to the excellent barrier properties of the skin. These drugs present molecular masses that are only up to a few hundred Daltons, exhibit octanol-water partition coefficients that heavily favor lipids, and require doses of no more than a few milligrams per day. It has been difficult to exploit the transdermal route to deliver hydrophilic drugs; the transdermal delivery of peptides and macromolecules, including new genetic treatments employing DNA or small-interfering RNA as in the case of vaccines, has posed particular challenges [10]. The use of energy sources as the driving force for drug transport across the skin, as well as the physical disruption of the more external layer of skin, constitutes the active approaches of permeability

enhancement, which enable the delivery of comparatively large quantities of drugs and biomacromolecules through the skin [5].

Structure of the Human Skin

Human skin is the largest organ of the body, covering about 1.7 m^2 and comprising approximately 10% of the total body mass. Its primary function is to provide a barrier between the body and the external environment. While the skin provides an ideal site for administration of therapeutic compounds for local and systemic effects, it presents a formidable barrier to the permeation of most compounds [11]. The knowledge of skin structure and function is fundamental for the design of transdermal dosage forms. Human skin, whose structure is shown in Fig. 1, is composed of three main regions:

Epidermis

The epidermis is a multilayered region whose cells lose viability with increasing distance from the basal layer. The epidermis is in a constant state of renewal, with the formation of a new cell layer of keratinocytes at the stratum basale and the loss of their nucleus and other organelles to form desiccated, proteinaceous corneocytes on their journey toward desquamation. Thus, the structure of the epidermal cells changes from the stratum basale through the stratum spinosum, stratum granulosum, and stratum lucidum (only present in palms and soles) to the stratum corneum. Epidermis possesses many enzymes capable of metabolizing topically applied compounds. Desmosomes act as molecular rivets, interconnecting the keratin of adjacent cells, thereby ensuring the structural integrity of the skin. In epidermis, Langerhans cells are antigen-presenting cells involved in the immune response; melanocytes produce the pigment melanin, whose function is to protect the skin by absorbing potentially harmful UV radiation.

The outermost layer of the epidermis, the stratum corneum (or horny layer), consists of 10–20μm of high density and low hydration cell layers. Although only 10–15 cells depth, it serves as the primary barrier of the skin, regulating water loss from the body and preventing permeation of potentially harmful substances and

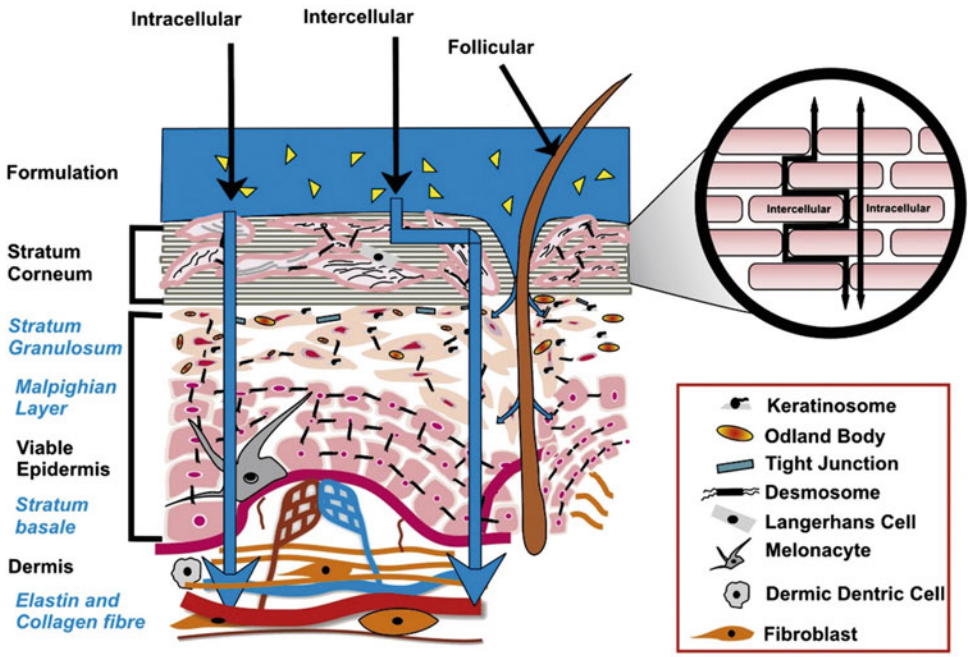

Transdermal Drug Delivery, Fig. 1 Diagrammatic representation of the skin structure along with the main penetration pathways. Reproduced with permission from Alexander et al. [12]

T

microorganisms from the skin surface. It has been described as a brick wall-like structure of corneocytes as "bricks" in a matrix (or "mortar") of intercellular lipids, with desmosomes acting as molecular rivets between the corneocytes. While this is a useful analogy, it is important to recognize that the corneocytes are elongated and flattened. The corneocytes lack of a nucleus and are composed of about 70%–80% keratin and 20% lipids within a cornified cell envelope (~10 nm thick). The unique composition of intercellular lipids and their structural arrangement in multiple lamellar layers within a continuous lipid domain are critical to the barrier function of the skin [11, 13].

Dermis and Appendages

The dermis is about 2–5 mm thick and consists of collagen fibrils that provide support and elastic connective tissue that provides elasticity and flexibility, embedded within a mucopolysaccharide matrix. Within this matrix is a sparse cell population, including fibroblasts that produce the components of the connective tissue (collagen, laminin, fibronectin, vitronectin) and mast cells, involved in immune and inflammatory responses. Due to this structure, the dermis provides little barrier to the permeation of most drugs but may reduce the permeation of very lipophilic drugs. It contains structures and appendages including blood and lymph vessels, nerve endings, hair follicles, and glands (sebaceous glands, eccrine, and apocrine sweat glands) [11, 14].

Subcutaneous Tissue

The subcutaneous tissue or hypodermis consists of a layer of fat cells arranged as lobules with interconnecting collagen and elastin fibers [11, 13].

Factors Affecting Skin Barrier Function

A number of physiological factors affect the skin barrier function and, as a result, its permeability. Even though aging alters the structure of all the skin layers including the stratum corneum, its barrier function is only affected in small children, where it is significantly reduced, particularly in neonates. Skin permeability varies with the anatomical site: while the highest absorption was seen for the scrotal areas (42 times greater than the ventral forearm), the lowest absorption was determined on the heel. There is little difference in skin barrier function between male and female skin. In women, however, during the menstrual cycle, skin barrier function is reduced in the days before the onset of menses. A number of skin diseases can compromise the barrier function of skin [11, 14].

Skin Permeation Pathways

When a substance is applied to the skin surface, there are two potential pathways to cross epidermis (see Fig. 1): through appendages (sweat ducts, hair follicles, and/or associated sebaceous glands) or through the continuous stratum corneum; both pathways are not mutually exclusive. It is considered that most compounds employ a combination of pathways. The relative contribution of each pathway is related to the physicochemical properties of the substance.

Appendages

Although it is accepted that the main permeation pathway is across the continuous stratum corneum, interest has arisen in the absorption through skin appendages, particularly through follicles. This can be achieved manipulating the formulation or modifying the target molecule. The formulation approximation includes pharmaceutical dosage forms based in particles, vesicles, and the use of sebum miscible excipients. Molecular modification involves optimizing physicochemical properties such as size, lipophilicity, solubility parameter, and charge [5, 11].

The Stratum Corneum

There are, in turn, two possible ways for permeation through the stratum corneum: intracellular (also known as transcellular) and intercellular routes. The former has been considered as a polar route through the stratum corneum. Since corneocytes contain an intracellular keratin matrix that is relatively hydrated (and, as a result, of polar nature), permeation requires successive partitions between this polar environment and the lipophilic

domains surrounding corneocytes. Current predominant view is, however, that transport through stratum corneum occurs mainly by the intercellular route.

Although lipid bilayers occupy only a small area of stratum corneum, they provide the only continuous route through this layer. The structure of stratum corneum lipids contributes to the barrier properties of skin. Within the intercellular lipid domains, transport can take place via both lipid (diffusion via the lipid core) and polar (diffusion via the polar head groups) pathways. Diffusion of very polar permeants occurs through, and is limited by, the polar pathway of the stratum corneum, being fairly independent of their partition coefficient. Less polar permeants are thought to diffuse via the lipid pathway, and permeation increases with an increase in their lipophilicity [5, 11].

Influence of the Physicochemical Characteristics of the Permeant

The diffusion coefficient or the speed at which a permeant moves within each environment depends on permeant properties like molecular size, solubility, melting point, ionization and the potential for binding within the environment, and factors related to the environment, such as its viscosity and tortuosity or diffusional path length. As the intercellular pathway is predominant, factors that influence movement within this environment are of major importance.

The first step in the skin transport process is partitioning of the permeant from the applied vehicle to the intercellular lipid domains of the stratum corneum, followed by diffusion within this relatively lipophilic environment. Increasing lipophilicity increases skin permeation, and it is considered that values between 1 and 3 are optimal for the logarithm of the octanol-water partition coefficient (log $P_{o/w}$). Very lipophilic molecules will have high solubility in the intercellular lipids but will not readily partition from the stratum corneum to the more aqueous viable epidermis, thus limiting their skin permeation rate. As a result, the ideal permeant requires lipid solubility but also a reasonable water solubility in order to maximize its flux.

The size and shape of the permeant substance will influence its diffusivity within the stratum corneum. It has been shown that there is an inverse relationship between molecular size of the permeant and skin penetration, and, as a general rule, the higher limit is 500 Da for conventional passive systems.

Increasing stratum corneum hydration increases skin permeability, and water is considered to be a natural skin penetration enhancer. This effect has been used in transdermal patches, occlusive dressings, and occlusive or hydrating topical formulations.

Permeation also depends on the degree of ionization which, in turn, affects the drug solubility in the formulation and its skin partition. The ionized species of a drug present lower permeability coefficients than their non-ionized counterparts. In this sense, the free acid or free base is generally used in order to improve permeation. However, the total flux of a permeant equals the sum of fluxes of all its ionized and non-ionized forms. The higher solubility in aqueous environments of ionized species can compensate, depending on the permeation pathways, the effect of their lower partition coefficient, resulting in comparable fluxes. Therefore, it is important to take into account both the formulation and the skin pH values [5, 11].

Permeation Enhancement

An ideal permeation enhancement would increase the skin permeability by a reversible disruption of the stratum corneum structure and/or by providing an additional driving force for the permeant transport across the skin, avoiding the damage of living deeper tissues. With this aim, different strategies have been developed and will be discussed below.

Passive Permeation Enhancement

The passive flux of a drug across a membrane is a function of its chemical potential gradient. Supersaturated phases allow achieving higher drug chemical potentials than those corresponding to

their solubility limit, increasing the drug flow. However, supersaturated states are thermodynamically metastable, and this could affect the shelf life of the formulation [15].

Another strategy consists in the use of chemical enhancers of permeation, that is, pharmacologically inactive compounds that can partition and diffuse in the membrane, interacting with stratum corneum components and promoting the drug flux. Although many penetration enhancers have been identified, only a few are safe for use and have been classified as GRAS (generally regarded as safe) by the US Food and Drug Administration (FDA). Recent developments in the field revealed highly potent yet safe enhancers or enhancer combinations, which suggest that enhancer-aided transdermal drug delivery has yet to reach its full potential [16].

Another strategy for permeation enhancement of charged drugs is the formation of ionic pairs, which are neutral species formed by the electrostatic attraction between opposite charge ions and are lipophilic enough to dissolve in an environment as the stratum corneum.

On the other hand, the reduction in the melting point of a permeant affects its solubility, increasing skin permeability. With this aim, deep eutectic solvents have been formed with propranolol, testosterone, ibuprofen, itraconazole, and lidocaine, among other drugs, and deep eutectic solvent vehicles were employed to solubilize drugs for transdermal delivery [17].

Permeation Enhancement by Physical Means

As it was mentioned previously, when the stratum corneum remains intact, the transdermal pathway of permeation is limited to molecules of relatively low molecular weight, neutral, and relatively lipophilic. In order to improve the transdermal bioavailability of peptides with therapeutical activity, proteins, vaccines, oligonucleotides, or drug-loaded particles, it is necessary to apply novel strategies. The purpose of a physical method of permeation enhancement is to increase not only the transdermal permeation rate of certain permeants but also to extend the range of permeating molecules as well, minimizing possible adverse reactions.

The physical methods of permeation enhancement can be combined with passive strategies and may be applied before or during the administration of the pharmaceutical dosage form. These can include the application of different forms of energy (heat, sound, light, electricity, magnetism) or the rupture, reduction, or weakening of the stratum corneum by mechanical means. The methods can be classified by their mechanism, according to their effect on the skin, as illustrated in Fig. 2.

Direct injection methods (e.g., with microneedles) pierce the stratum corneum to deliver an active substance at a predetermined depth. These systems have been called "minimally invasive."

Mechanical techniques such as adhesive tape stripping or microdermabrasion partially improve penetration as they reduce stratum corneum thickness, while flexion or stretching can cause a general weakening of the barrier. Massage can also promote follicular pathway administration, especially in the case of drug-loaded microparticles, in order to create a follicular reservoir.

Ablative or cavitational technologies eliminate the stratum corneum in specific points, forming micropores of microchannels through which diffusion occurs. Examples of these techniques are thermal ablation, laser, radiofrequency (RF), ultrasound, and electroporation, among others.

Lastly, there are technologies such as non-cavitational ultrasound, dermaportation (magnetophoresis), and iontophoresis, whose purpose is to increase penetration by increasing the driving force applied to the permeant [11].

Microneedles, as the name suggests, consist of micron-sized projections similar to needles, which may vary from 100 to 1000μm in length. They are capable of piercing the skin through the stratum corneum but fail to reach the nerve endings due to their small size and thus do not elicit pain. Tremendous work has been conducted for the production of microneedles composed of a wide range of materials, from polymers to metals, using varied fabrication techniques. Microneedles can be classified in different types: solid, hollow, coated, dissolvable/biodegradable/hydrogel forming,

Transdermal Drug Delivery,
Fig. 2 Penetration of topically applied substances through untreated skin and following three different treatments: direct injection, barrier reduction, and cavitational technologies

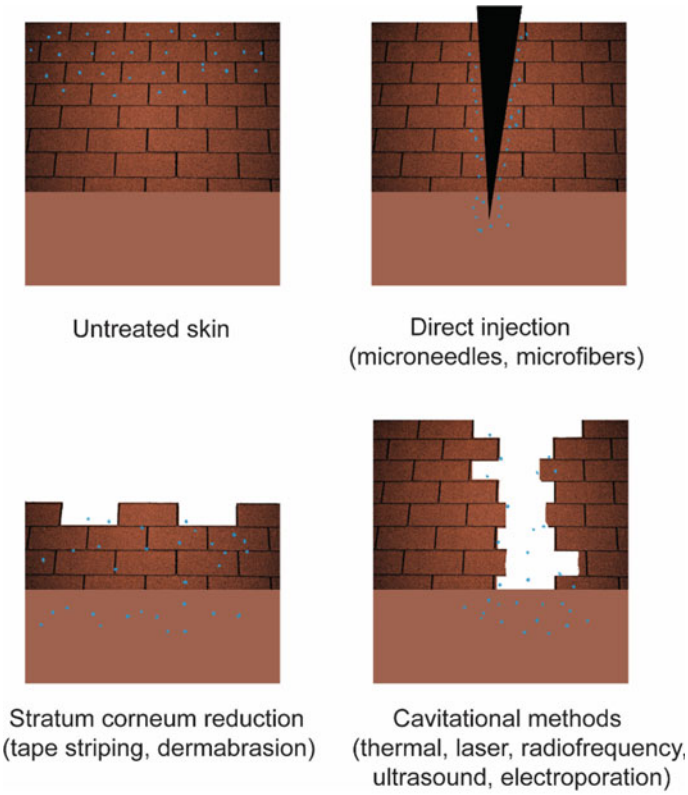

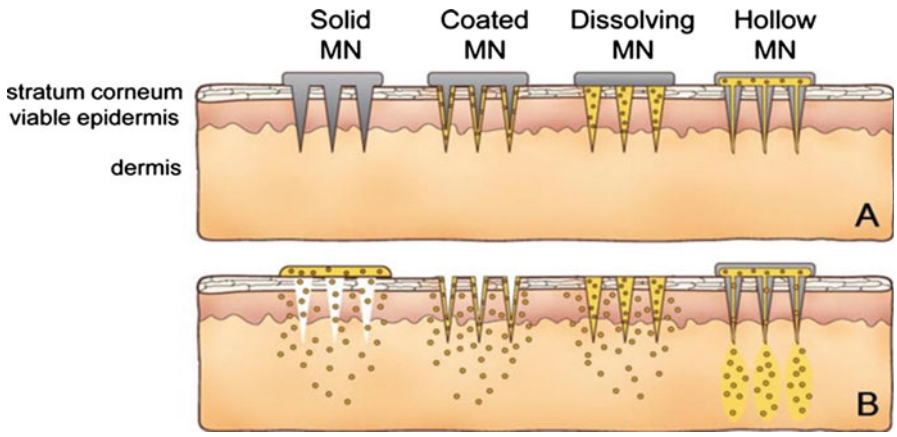

Transdermal Drug Delivery, Fig. 3 Representation of transdermal drug delivery with different types of microneedles. Solid microneedles are used as a pretreatment. Reproduced with permission from Kim et al. [19]

and rapidly separating microneedles [18]. Drug release from microneedles is illustrated in Fig. 3, and micrographs of hollow microneedles are shown in Fig. 4.

Iontophoresis is a technique that involves the application of low current intensities (usually less than 0.5 mA/cm^2) to the skin, to enhance the topical and transdermal delivery of both charged

T

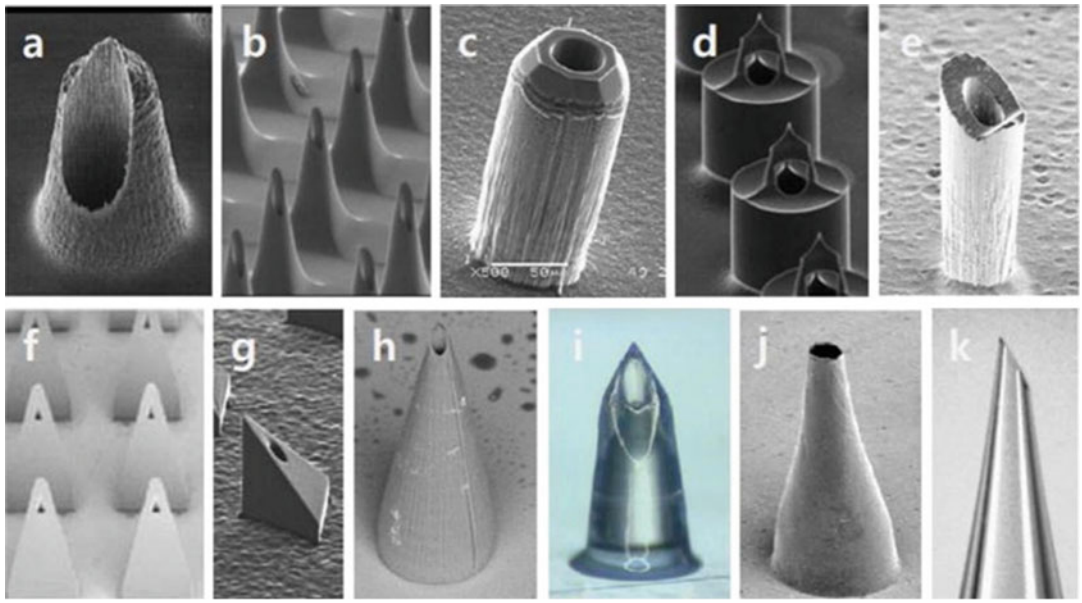

Transdermal Drug Delivery, Fig. 4 Example micrographs of hollow microneedles made of silicon (**a**-**e** and **g**-**k**) or poly(methyl methacrylate) (**f**). Reproduced with permission from Kim et al. [19]

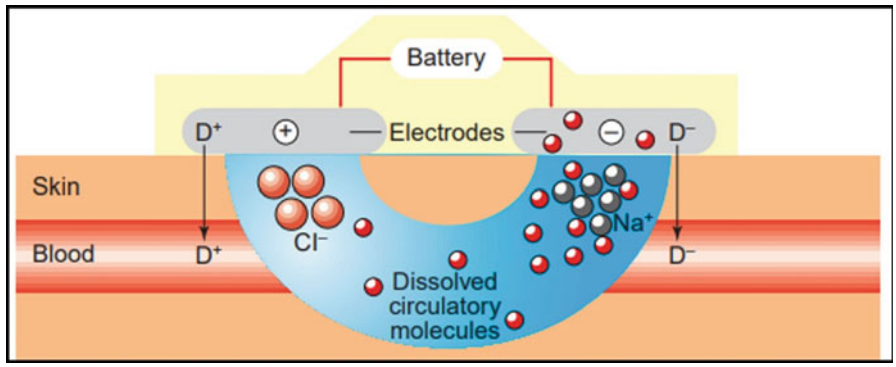

Transdermal Drug Delivery, Fig. 5 Basic principle behind iontophoretic drug delivery. D^+ and D^- represent positively and negatively charged drug molecules, respectively. The electrode on the left is the anode (positively charged), and the one on the right is the cathode (negatively charged). Reproduced with permission from Naik et al. [22]

and neutral molecules. The application of a current through electrodes results in the electromigration of charged drug molecules, causing them to be driven through the skin (Fig. 5). The movement of the drug molecules is accompanied by the flow of water, which is known as electroosmosis.

The transport of neutral molecules also occurs at the anode by electroosmosis along with the bulk water flow from anode to cathode. The isoelectric point of the human skin is around 4–4.5, which is below the pH of physiological conditions (pH 7.4). Therefore, skin is negatively charged, which favors the flow of water from anode to cathode. Endogenous counterions migrate to close the circuit.

Thus, iontophoresis enables transport of several hydrophilic drugs that cannot otherwise be

delivered passively. Also, the flow of electric current may enhance the permeability of the skin. The two main advantages of iontophoresis are the wider range of drugs that can be administered (up to 15 kDa) and the possibility of modulation of the rate and profile of drug delivery, allowing pulsatile or on-demand bolus administration, among other complex delivery kinetics.

Although iontophoresis has a longer history, prefilled iontophoretic systems are more recent and are a result of the advances in microelectronics, of the success of passive transdermal patches, and of the need of noninvasive administration methods for therapeutic peptides and proteins of recombinant DNA technology origin [20, 21].

A typical prefilled iontophoretic delivery system consists of a microprocessor, a current source, and two electrodes. The drug reservoir is placed under the appropriate electrode, while the other electrode serves as a counter electrode to complete the circuit. Negatively charged species (as D^- in Fig. 5) are propelled into the skin under the influence of cathode, and positively charged ions (D^+) are transferred through the skin under the influence of anodal delivery. In iontophoretic systems, drug delivery depends on the duration and intensity of the current applied and also on the drug content in the formulation, the pH that defines drug ionization, and the patch application area [20].

Some successful examples of the application of iontophoresis for systemic drug delivery include the administration of fentanyl HCl (opioid) for patient-controlled pain management (Fig. 6), the administration of alniditan and sumatriptan for the treatment of migraine, the administration of tacrine, a reversible acetylcholinesterase inhibitor useful for the treatment of neurodegenerative diseases, the administration of R-apomorphine, a dopaminergic agonist, in patients with idiopathic Parkinson disease and the administration of metoclopramide as an antiemetic agent. Iontophoresis has also been employed for the noninvasive administration of peptides and proteins including luteinizing hormone-releasing hormone (LHRH), calcitonin, growth hormone-releasing hormone, human parathyroid hormone, and insulin for diabetes management [11].

Classification of Transdermal Systems

From a global perspective, transdermal systems have been divided in four generations:

First-Generation Systems

This generation encompasses most of the transdermal patches currently in clinical use. These systems do not take advantage of physical or chemical skin permeability enhancement, and as a result, they are limited to drugs with suitable physicochemical properties.

A variation on the traditional transdermal patch of first-generation delivery systems involves no patch at all but applies a metered liquid spray, gel, or other topical formulation to the skin that, upon evaporation or absorption, can drive small lipophilic drugs into the stratum corneum, which in turn serves as the drug reservoir for an extended release into the viable epidermis over hours. Examples of these systems are testosterone and estradiol gels, as well as clotrimazole sprays [9, 24].

Second-Generation Systems

These systems employ skin permeability enhancement to expand the scope of transdermal drugs. However, enhancement methods developed in this generation, such as conventional chemical enhancers, iontophoresis, and noncavitational ultrasound, have struggled with the balance between achieving increased delivery across stratum corneum, while protecting deeper tissues from damage. As a result, this second generation of delivery systems has advanced to clinical practice primarily by improving small-molecule delivery for localized, dermatological, cosmetic, and some systemic applications but has made little clinically important effect on the delivery of macromolecules.

Within this generation are systems that include a variety of nanocarriers including liposomes, dendrimers, and nano/microemulsions, as chemical enhancers with supramolecular structure that can increase not only skin permeability, but also drug solubilization in the formulation and drug partitioning into the skin.

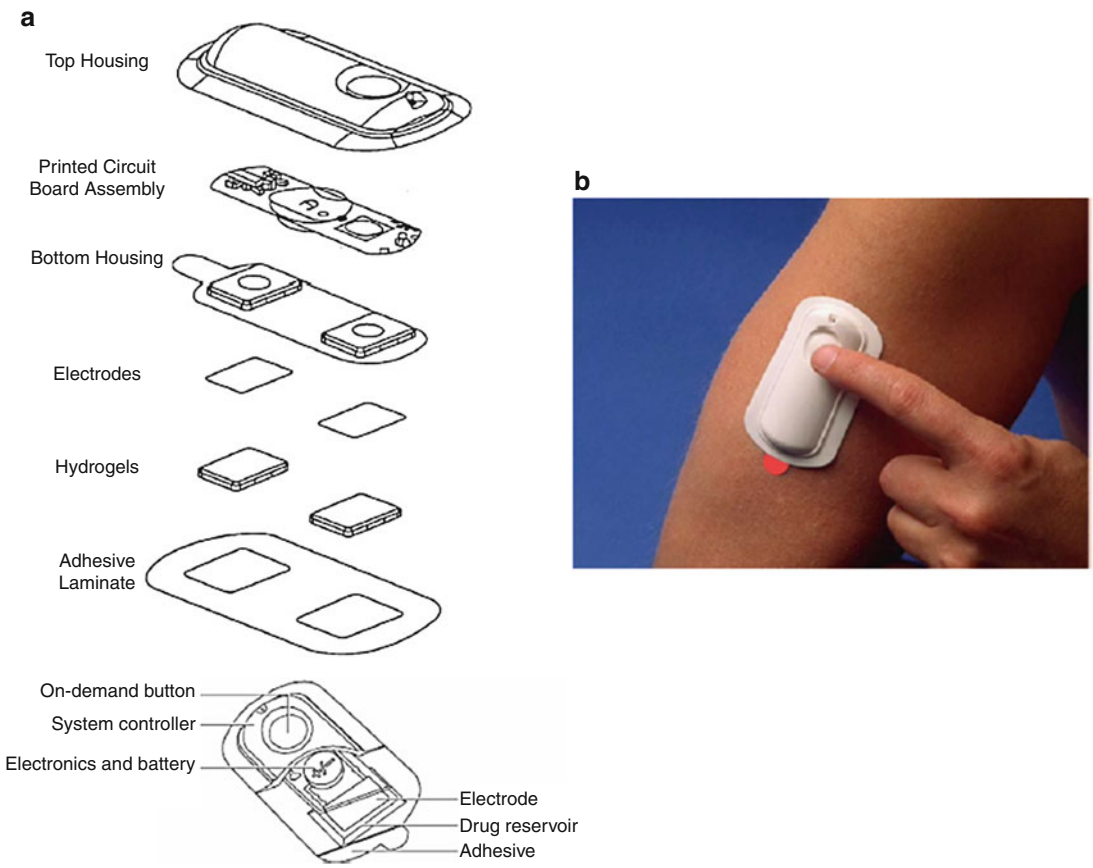

Transdermal Drug Delivery, Fig. 6 (**a**) Internal scheme of an iontophoretic fentanyl HCl delivery system showing major components, (**b**) the drug delivery from the iontophoretic patch applied onto the upper arm skin is initiated by the patient using the controller button. Reproduced with permission from Subramony et al. [23]

Another approach that has been applied in this generation is the use of prodrugs, which are pharmacological inactive derivatives of a drug molecule. Through the addition of a cleavable chemical group that typically increases drug lipophilicity, such prodrugs can facilitate the transfer of a drug across the skin. The drug is later recovered, due to enzymatic or chemical cleavage in the body. One prodrug approach relies on the linkage of either two of the same or two different small-molecule drugs to each other by a labile bond, which reduces their hydrophilicity, albeit at the expense of increasing molecular weight [9, 24, 25].

Third-Generation Systems

The third generation of transdermal delivery systems is poised to have a large impact on drug delivery because it targets its effects to the stratum corneum. This targeting enables stronger disruption of the stratum corneum barrier, and thereby more effective transdermal delivery, while still protecting deeper tissues. In this way, novel chemical and biochemical enhancers, electroporation, cavitational ultrasound, and, more recently, microneedles, thermal ablation, and microdermabrasion have been able to deliver macromolecules, including therapeutic proteins and vaccines, across the skin in human clinical trials [9, 24, 26].

Fourth-Generation Systems

Personalized therapy allows to optimize a treatment based on the patient pathophysiological conditions. This kind of therapy requires systematic

control of the administered dose based on an accurate real-time observation of the physiological parameters, in order to determine the progression of disease and efficacy of the drug. In this sense, the next generation of transdermal systems has been proposed. Rapid advances in soft and ultrathin devices in wearable forms have facilitated the seamless integration of bioelectronic devices into a skin-mounted patch domain with unprecedented functionalities. In fourth-generation systems, sensors accurately measure the physiological, electrophysiological, and biochemical signals, actuators transfer energy to the drug-loaded patch in a controlled manner, and the sensors subsequently gather information on the therapeutic efficacy of the drug. The synergetic performance of wearable devices and drug delivery patches according to a complete feedback loop provides a novel platform for personalized therapy. This approach has been investigated to treat diabetes and thrombosis [23, 24].

Structure of Transdermal Passive Noninvasive Patches

In the nearly five decades of experience with current transdermal patches, there has been an evolution in the spatial disposition of the different components inside their structure (Fig. 7). The design of passive transdermal patches (first-generation and some second-generation systems) is characterized by a multi-layered structure that usually presents three or four basic elements: an impermeable backing film, a formulation containing the drug together with excipients, an adhesive that reversibly fixes the patch to the skin, and a protective release liner that is peeled off before being applied. Patches currently in use are mainly *reservoir with rate-controlling membrane* and *drug in adhesive* systems, with the latter being predominant in the last years [3].

In recent years, the structure of transdermal systems has become more complex and in the case of active patches may include sensors, electrodes, electronic circuits, and electrical batteries, as well as microneedles in the minimally invasive patches, as has been pointed out previously [24, 27].

Reservoir Systems with Rate-Controlling Membrane

The first of these systems was a combination of a reservoir containing the drug (initially scopolamine) and a rate controlling membrane. In this type of patch design (Fig. 7a), the drug is included generally in a compartment, in liquid form (in solution or suspension), or in a gel. The reservoir is separated of the continuous adhesive layer by a permeable membrane that controls the release of the drug, thus reducing the variability in skin permeability among individuals. In this initial

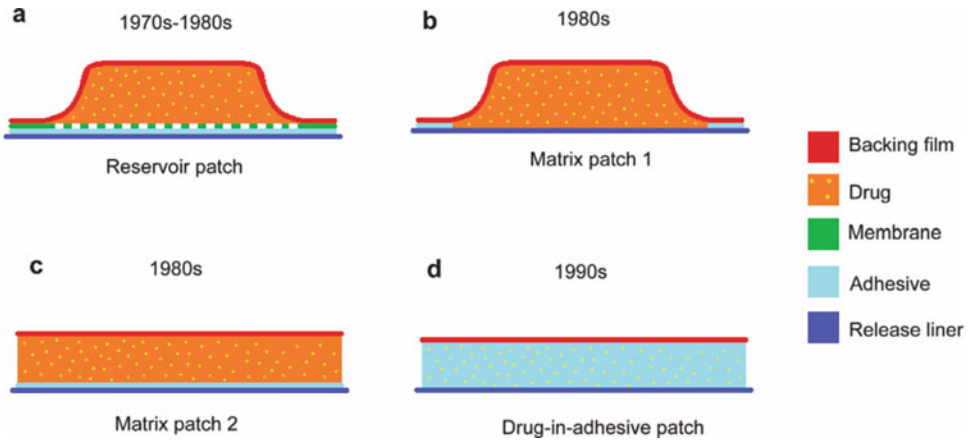

Transdermal Drug Delivery, Fig. 7 **(a–d)** Evolution in the spatial disposition of components in passive noninvasive patches currently available in the market

design, the drug equilibrates with the adhesive layer acting as a prime dose that can saturate the skin binding sites, which can be an advantage or disadvantage depending on the specific therapeutic needs.

The main advantage of reservoir type patches with membranes is that, in some cases, they present a constant release speed (zero-order kinetics). However, as the membrane rate control is increased, this design requires a bigger size in order to achieve the drug delivery. An important limitation of this design is the potential drug leak from the sealed liquid reservoir, which can result in an overdose [3, 28].

Matrix Patches

In the 1980s, matrix designs (Fig. 7b, c) became the dominant products in the transdermal systems market. This was not only due to the fact that these patches were thinner, flexible, and more comfortable to wear, but also their manufacture was less expensive. In general, all devices that do not contain a liquid reservoir can be considered matrix patches and can be applied to the skin by means of an adhesive that forms a ring around the matrix or a continuous film between the matrix and the skin. The patches in which the drug is incorporated into a polymeric or viscous adhesive, which are described in the next section, are also matrix systems. Depending on the design, these systems can provide a zero-order release kinetics [3].

Drug in Adhesive Patches

Patches with drug in the adhesive simply incorporate the drug in the pressure-sensitive adhesive which also controls the release rate (Fig. 7d). This design, which is also a matrix type, constitutes the simpler (and the newer) of passive patches designs and has become the industry standard. Drugs such as clonidine, haloperidol, nitroglycerin, dihydroergotamine, or fentanyl have been successfully incorporated in adhesive patches (e.g., of acrylic type, silicones, or polyisobutylene). However, while these patches seem to be easier to manufacture than other traditional designs, the formulation of the drug in the adhesive may be complex.

Drug in adhesive patches are even lighter, thinner, more flexible, and comfortable to wear, they adapt better to skin surface variations and considerably improve patient acceptance. However, an important disadvantage is that if the drug is completely soluble, its release speed from the device depends on its concentration in the adhesive (first-order kinetics), thus bringing about a decrease in the release rate with wear time. As a result, a constant release rate can be achieved, when the drug is in solution, only if at least 80% of the drug remains in the patch when this is removed. Another alternative for achieving constant release is to use the drug in suspension [3, 29].

Cross-References

▶ Permeation Enhancers

References

1. European Pharmacopoeia 10th Ed. Strasbourg: European Pharmacopoeia Commision; 2020.
2. The United States Pharmacopeia 43. Rockville: United States Pharmacopeia Convention; 2020.
3. Pastore MN, Kalia YN, Horstmann M, Roberts MS. Transdermal patches: history, development and pharmacology. Br J Pharmacol. 2015;172:2179–209. https://doi.org/10.1111/bph.13059.
4. Price NM, Schmitt LG, McGuire J, Shaw JE, Trobough G. Transdermal scopolamine in the prevention of motion sickness at sea. Clin Pharmacol Ther. 1981;29:414–9. https://doi.org/10.1038/clpt.1981.57.
5. Akhtar N, Singh V, Yusuf M, Khan RA. Non-invasive drug delivery technology: development and current status of transdermal drug delivery devices, techniques and biomedical applications. Biomed Eng/Biomed Tech. 2020;65:243–72. https://doi.org/10.1515/bmt-2019-0019.
6. The Business Research Company. Transdermal skin patches market global report 2020–30. https://www.researchandmarkets.com/. Accessed 17 Dec 2020.
7. Mayes S, Ferrone M. Fentanyl HCl patient-controlled iontophoretic transdermal systems for the management of acute postoperative pain. Ann Pharmacother. 2006;40:2178–85. https://doi.org/10.1345/aph.1H135.
8. Kennedy J, Larrañeta E, McCrudden MTC, McCrudden CM, Brady AJ, Fallows SJ, et al. In vivo studies investigating biodistribution of nanoparticle-encapsulated rhodamine B delivered via dissolving

micro needles. J Control Release. 2017;265:57–65. https://doi.org/10.1016/j.jconrel.2017.04.022.
9. Prausnitz MR, Langer R. Transdermal drug delivery. Nat Biotechnol. 2008;26:1261–8. https://doi.org/10.1038/nbt.1504.
10. Foldvari M, Babiuk S, Badea I. DNA delivery for vaccination and therapeutics through the skin. Curr Drug Deliv. 2005;3:17–28. https://doi.org/10.2174/156720106775197493.
11. Benson HAE, Watkinson AC. Topical and transdermal drug delivery. Hoboken: Wiley; 2011. https://doi.org/10.1002/9781118140505.
12. Alexander A, Dwivedi S, Ajazuddin GTK, Saraf S, Saraf S, et al. Approaches for breaking the barriers of drug permeation through transdermal drug delivery. J Control Release. 2012;164:26–40. https://doi.org/10.1016/j.jconrel.2012.09.017.
13. Moss P. Introduction. In: Donnelly R, Singh T, editors. Novel delivery systems for transdermal and intradermal drug delivery. Chichester: Wiley; 2015. p. 1–40.
14. Thakur R, Batheja P, Kaushik D, Michniak B. Structural and biochemical changes in aging skin and their impact on skin permeability barrier. In: Skin aging handbook. Norwich: William Andrew Publishing; 2009. p. 55–90.
15. Hirakawa Y, Ueda H, Miyano T, Kamiya N, Goto M. New insight into transdermal drug delivery with supersaturated formulation based on co-amorphous system. Int J Pharm. 2019;569 https://doi.org/10.1016/j.ijpharm.2019.118582.
16. Kováčik A, Kopečná M, Vávrová K. Permeation enhancers in transdermal drug delivery: benefits and limitations. Expert Opin Drug Deliv. 2020;17:145–55. https://doi.org/10.1080/17425247.2020.1713087.
17. Emami S, Shayanfar A. Deep eutectic solvents for pharmaceutical formulation and drug delivery applications. Pharm Dev Technol. 2020;25:779–96. https://doi.org/10.1080/10837450.2020.1735414.
18. Dharadhar S, Majumdar A, Dhoble S, Patravale V. Microneedles for transdermal drug delivery: a systematic review. Drug Dev Ind Pharm. 2019;45:188–201. https://doi.org/10.1080/03639045.2018.1539497.
19. Kim YC, Park JH, Prausnitz MR. Microneedles for drug and vaccine delivery. Adv Drug Deliv Rev. 2012;64:1547–68. https://doi.org/10.1016/j.addr.2012.04.005.
20. Bakshi P, Vora D, Hemmady K, Banga AK. Iontophoretic skin delivery systems: success and failures. Int J Pharm. 2020;586:119584. https://doi.org/10.1016/j.ijpharm.2020.119584.
21. Kanikkannan N, Bonner M, Singh J, Roberts M. Iontophoresis. In: Walters K, Roberts M, editors. Dermatologic, cosmeceutic and cosmetic development: therapeutic and novel approaches. New York: Informa Healthcare; 2007. p. 517–35.
22. Naik A, Kalia YN, Guy RH. Transdermal drug delivery: overcoming the skin's barrier function. Pharm Sci Technol Today. 2000;3:318–26. https://doi.org/10.1016/S1461-5347(00)00295-9.
23. Subramony JA, Sharma A, Phipps JB. Microprocessor controlled transdermal drug delivery. Int J Pharm. 2006;317:1–6. https://doi.org/10.1016/j.ijpharm.2006.03.053.
24. Lee H, Song C, Baik S, Kim D, Hyeon T, Kim DH. Device-assisted transdermal drug delivery. Adv Drug Deliv Rev. 2018;127:35–45. https://doi.org/10.1016/j.addr.2017.08.009.
25. Rabiei M, Kashanian S, Samavati SS, Jamasb S, McInnes SJP. Nanomaterial and advanced technologies in transdermal drug delivery. J Drug Target. 2020;28:356–67. https://doi.org/10.1080/1061186X.2019.1693579.
26. Lim DJ, Vines JB, Park H, Lee SH. Microneedles: a versatile strategy for transdermal delivery of biological molecules. Int J Biol Macromol. 2018;110:30–8. https://doi.org/10.1016/j.ijbiomac.2017.12.027.
27. Lee HJ, Choi N, Yoon ES, Cho IJ. MEMS devices for drug delivery. Adv Drug Deliv Rev. 2018;128:132–47. https://doi.org/10.1016/j.addr.2017.11.003.
28. Oliveira G, Hadgraft J, Lane ME. Toxicological implications of the delivery of fentanyl from gel extracted from a commercial transdermal reservoir patch. Toxicol Vitr. 2012;26:645–8. https://doi.org/10.1016/j.tiv.2012.02.007.
29. Padula C, Nicoli S, Aversa V, Colombo P, Falson F, Pirot F, et al. Bioadhesive film for dermal and transdermal drug delivery. Eur J Dermatology. 2007;17:309–12. https://doi.org/10.1684/ejd.2007.0205.

Transdermal Enhancers

▶ Permeation Enhancers

Transdermal Patches

▶ Transdermal Drug Delivery

Transport-Controlled Dissolution

▶ Drug Dissolution: Fundamental Theoretic Models

Transporter Drug Interactions

Robert Elsby[1], Philip Butler[2] and Robert J. Riley[2]
[1]Department of ADME Sciences, Cyprotex Discovery Ltd (an Evotec company), Cheshire, UK
[2]Cyprotex Discovery Ltd (an Evotec company), Cheshire, UK

Definition

Drug transporters are membrane-bound cellular proteins that act as gatekeepers to facilitate either (1) the entry or (2) the exit of endobiotics or xenobiotics (drugs), into or out of cells, respectively. Two superfamilies exist, the ATP-binding cassette (ABC) transporter family, which is responsible for efflux out of cells, and the solute carrier (SLC) transporter family that primarily uptake into cells. Together these transporters can influence the intracellular concentrations of drugs within tissues which, in turn, can impact both their efficacy and toxicity. Furthermore, due to their expression on enterocytes of the gastrointestinal tract, on hepatocytes, at the blood-brain barrier, and on renal proximal tubule cells, transporters can determine pharmacokinetics by modulating the absorption, distribution, metabolism, and elimination (ADME) of drugs that are substrates.

Mechanistic changes in these ADME processes, and subsequently in the pharmacokinetic profile of a substrate drug, can occur when it is co-administered with another drug that interacts (as an inhibitor/inducer) with the same transporter(s). Such occurrences are referred to as "transporter-mediated drug-drug interactions (DDIs)," for which the term "victim" is applied to the substrate drug whose pharmacokinetic exposure (area under the curve, AUC, and maximum plasma concentration, C_{max}) is increased upon co-administration of a second "perpetrator" drug which inhibits the transporter(s) responsible for the victim's disposition. Additionally, more complex DDIs can occur and can exacerbate the transporter-mediated impact if the victim drug's principal ADME pathways also involve metabolizing enzymes that are equally susceptible to inhibition by the same perpetrator drug clinically.

Knowledge of the clinically significant DDIs for a marketed drug is required for the drug's label, or summary of product characteristics, in order to guide physician-led decisions around dosing patients safely during clinical use.

Drug Transporters

ATP-Binding Cassette (ABC) Transporters

ABC transporters are a superfamily of efflux proteins expressed at barrier and excretion membranes that play a protective role by pumping xenobiotics/drugs out of cells. These energy-dependent transporters are of the type "primary active," which generate the energy required for transport themselves through the hydrolysis of ATP to ADP and inorganic phosphate as part of an integrated ATPase cycle. As a transporter, they transport in one direction only and move (efflux) a substrate against its concentration gradient. There are approximately fifty ABC transporters in seven subfamilies (denoted by letter), but of these, only two transporters (P-glycoprotein and breast cancer resistance protein) are currently deemed (from a regulatory authority standpoint) to have a critical role in the clinical disposition and observed clinically significant DDIs of common co-medications [1].

P-glycoprotein (P-gp; ABCB1) P-glycoprotein (P-gp; synonym multidrug resistance protein 1, MDR1) is a member of the ABC "B" subfamily (ABCB1), and its membrane structure consists of two 6-membrane-spanning domains and two nucleotide-binding domains that bind and hydrolyze ATP. The transporter is ubiquitously expressed on the brush border (apical) membrane of enterocytes, the canalicular membrane of hepatocytes, the brush border (apical) membrane of renal proximal tubular cells, and the endothelial cells of the blood-brain barrier [1]. Consequently, P-gp efflux at these sites can affect the oral absorption, biliary and renal clearance, and/or brain penetration of drugs that are substrates of this transporter. If a drug is subject to significant P-gp efflux, its absorption, distribution, (metabolism), and elimination (ADME) could be altered

by potent P-gp inhibitors, resulting in toxicity or altered efficacy.

Breast Cancer Resistance Protein (BCRP; ABCG2) Breast cancer resistance protein (BCRP) is a member of the ABC "G" subfamily (ABCG2) and, unlike P-gp, is a "half" transporter protein consisting of a single 6-membrane-spanning domain and a single ATP-binding domain, which dimerizes with another half transporter to function. Similar to P-gp, BCRP is ubiquitously expressed in the intestine (apical brush border membrane of enterocytes), liver (canalicular membrane of hepatocytes), and kidney (apical brush border membrane of renal proximal tubule cells) and can therefore affect the absorption and elimination of drugs that are substrates of this transporter, ultimately defining their pharmacokinetic exposure [1, 2]. Indeed, clinical pharmacogenetic studies have demonstrated that individuals exhibiting impaired BCRP functional capability, due to a single-nucleotide polymorphism (c.421C.A) in the gene (*ABCG2*) encoding the transporter, had higher plasma levels of several BCRP substrate drugs including rosuvastatin, atorvastatin, fluvastatin, and diflomotecan due to their increased absorption [3, 4]. Furthermore, it has been reported that the observed ethnic difference and variability in the exposure of the BCRP substrates rosuvastatin and atorvastatin between Caucasian and Asian populations can be explained by the higher frequency of the *ABCG2* c.421C.A polymorphism in Asian populations resulting in their higher absorption of such BCRP substrate drugs due to impaired BCRP efflux [4, 5]. Interestingly, this pharmacogenetic effect between individuals of the same ethnicity, with differing BCRP functional phenotype, gives insight into how the absorption and elimination of specific substrate drugs could be altered by potent BCRP inhibitors in clinical practice, resulting in their toxicity or altered efficacy.

Solute Carrier (SLC) Transporters

SLC transporters are a superfamily of uptake/influx proteins ubiquitously expressed at membranes of tissues and organs throughout the body and are responsible for maintaining cell homeostasis and nutrient distribution by transporting endobiotics into cells [6]. Some SLC transporter subfamilies (e.g., the organic cation transporters, OCTs) are "passive facilitative" transporters that do not use energy to transport a substrate into cells; rather, they act as cell gatekeepers for a substrate to move by passive diffusion down its concentration gradient. The remaining SLC transporter subfamilies are of the type "secondary active," which utilize the free energy derived from voltage/ion gradients generated by a separate primary active transporter (such as a sodium/potassium ATPase) or electrochemical gradient, in order to drive their transport of molecules across cell membranes. This is achieved by coupling the cotransport of the ion with the intended substrate, either in the same direction (performed by cotransporters or symporters) or in opposite directions (performed by exchangers or antiporters) [6]. SLC transporters are able to transport in both directions, but only the active transporters are able to move a substrate against its concentration gradient. Substrates of SLC transporters are typically charged (positive = cation; negative = anion), hydrophilic (water-preferring) molecules, and in addition to endobiotics, they also include various drugs (xenobiotics). There are approximately 458 SLC transporters in 65 subfamilies (denoted by number), but of these, only 8 transporters (organic anion transporting polypeptides 1B1 and 1B3, organic anion transporters 1 and 3, organic cation transporters 1 and 2, and multidrug and toxin extrusion 1 and 2-K) are currently deemed to have a critical role in the clinical disposition and observed clinically significant DDIs of common co-medications (from a regulatory authority standpoint) [1].

Hepatic SLC Transporters Organic anion transporting polypeptides 1B1 (OATP1B1) and 1B3 (OATP1B3) are members of the SLCO subfamily (SLCO1B1 or SLCO1B3, respectively) and have predicted membrane structures consisting of 12 membrane-spanning domains. These transporters are uniquely expressed in the liver on the basolateral membrane of hepatocytes and are responsible for the uptake of a broad range

of endogenous anionic compounds including bile acids and sulfate and glucuronide conjugates, as well as of various drug substrates (e.g., statins, sartans). The uptake by these transporters can often be the rate-limiting step in a drug's hepatic elimination/clearance [7]. Similar to BCRP, clinical pharmacogenetic studies have also demonstrated that individuals exhibiting reduced OATP1B1 functional capability, due to a single-nucleotide polymorphism (c.521T.C) in the gene (*SLCO1B1*) encoding the transporter, had higher plasma levels of several OATP1B1 substrate drugs including simvastatin acid, pitavastatin, atorvastatin, pravastatin, rosuvastatin, repaglinide, and olmesartan due to their decreased active hepatic elimination on first pass [1, 3, 4]. These clinical observations highlight how the elimination of specific substrate drugs could be altered by potent OATP1B1 inhibitors in the clinic, resulting in their toxicity (e.g., myopathy in the case of statins) or altered efficacy. Organic cation transporter 1 (OCT1), a member of the SLC22A subfamily (SLC22A1), is another important hepatic uptake transporter involved in the disposition of cationic drugs such as fenoterol (for which OCT1 is the rate-limiting step in elimination based on clinical pharmacogenetic studies [8]) and metformin (for which OCT1 controls entry to the target site of action), such that inhibition in the clinic by a co-administered drug could result in their toxicity or altered efficacy.

Renal SLC Transporters Organic anion transporters 1 (OAT1) and 3 (OAT3) and organic cation transporter 2 (OCT2) are members of the SLC22 subfamily (SLC22A6, SLC22A8, and SLC22A2, respectively) and have similar membrane structural features comprising 12 transmembrane domains [6]. These uptake transporters are expressed on the basolateral membrane of renal proximal tubule cells and are involved in the active renal secretion of a range of endogenous anions or cations (e.g., creatinine) in addition to drugs such as antibiotics (e.g., ciprofloxacin; OAT1/3), antirheumatics (e.g., methotrexate; OAT1/3), hydrophilic statins (e.g., pravastatin and rosuvastatin; OAT3), antivirals (e.g., acyclovir; OAT1), diuretics (e.g., furosemide; OAT3), antiarrhythmics (e.g., procainamide; OCT2), and antidiabetics (e.g., metformin; OCT2). Once inside the proximal tubule cell, the molecules above require transporter-mediated efflux across the brush border membrane in order to complete their active renal elimination. For cationic drugs, this process is predominantly performed by members of the SLC47 subfamily, namely, multidrug and toxin extrusion 1 (MATE1; SLC47A1) and 2-K (MATE2-K; SLC47A2), which have similar membrane structures to the other renal SLC transporters above. Inhibition of any of these SLC22 or SLC47 transporter proteins in the clinic could result in delayed renal elimination and increased potential for toxicity of substrate drugs.

Transporter Drug-Drug Interactions

Intestinal Transporter-Mediated Interactions

P-gp

Clinically significant DDIs attributed to inhibition of P-gp-mediated transport are described in Table 1. To date, because of its narrow therapeutic index and ensuing toxicity if plasma levels are elevated above the normal therapeutic range, most described P-gp-mediated DDIs concern the cardiac glycoside digoxin as the victim drug. Digoxin is susceptible to pharmacokinetic perturbations (theoretical maximum 1.43-fold increase in AUC) as a result of inhibition of P-gp because P-gp efflux plays a critical role in both attenuating its absorption and in its active renal elimination. However, while the majority of early studies attributed decreased P-gp-mediated renal clearance of digoxin (↓ approx. 30%) as the mechanism underlying observed DDIs, it was apparent in the study of Pedersen et al. [9] and in more recent studies [10–12], and from scrutinizing available reported AUC profiles with and without co-administered inhibitor in earlier studies, that the actual mechanism causing DDI is in fact decreased P-gp-mediated intestinal efflux resulting in increased absorption of digoxin (↑ approx. 30%; from usual 70 to 100%). Evidence for enhanced oral bioavailability is supported by the increase in maximum plasma concentrations

and AUC of digoxin observed in pharmacokinetic profiles, in the absence of a change in time to maximal peak concentration or a change in half-life and elimination phase (representing renal clearance), which remained parallel with and without inhibitor drug. Any "apparent" decrease in digoxin renal clearance (derived from the amount of digoxin in urine divided by AUC) was merely an artifact reflecting an increased amount of digoxin present in the urine as a consequence of the individuals absorbing more digoxin into the body.

BCRP

Clinically significant DDIs attributed to inhibition of BCRP-mediated transport are described in Table 1 and involve low-permeability substrate drugs for whom intestinal BCRP efflux is the rate-determining step that limits their absorption [2]. Such sensitive drugs include topotecan [13], rosuvastatin, atorvastatin, or fluvastatin [14, 15], giving maximum theoretical fold increases in plasma exposure (AUC) of 2.4-, 2-, 1.72-, or 1.72-fold, as a result of increasing the drug's overall absorption from 40 to 97%, 50 to 100%, 40 to 69%, or 58 to 100% when BCRP is inhibited, respectively. Conversely, the magnitude of exposure increases due to BCRP-mediated DDI will be significantly lower, or negligible, in individuals who express an impaired BCRP pharmacogenetic phenotypic variant (c.421 AC or c.421AA) because they have less functional BCRP to inhibit by perpetrator drug. It is important to note that ADME pathways other than intestinal BCRP may also contribute towards manifesting DDIs for atorvastatin (CYP3A4 and OATP1B1), fluvastatin (CYP2C9), and rosuvastatin (OATP1B1, OAT3) [14], although for the latter, the majority of DDIs reported on the drug's label can be solely attributed to inhibition of intestinal BCRP as the mechanism [15].

Hepatic Transporter-Mediated Interactions

OATP1B1

Clinically significant DDIs attributed to inhibition of OATP1B1-mediated transport are described in Table 1 and typically involve low-permeability substrate drugs for whom hepatic transporter uptake is the rate-determining step in their hepatic elimination, which in turn is the major clearance pathway that affects the drug's pharmacokinetics [7]. Such sensitive OATP1B1 substrate drugs include the statin common co-medications, for which inhibition of OATP1B1 alone (in the absence of other pathways) would result in a $<$ five-fold increase in plasma exposure (AUC) of the statin with the following rank order of theoretical maxima based on the fraction excreted (f_e) value of the transporter for the specific statin: simvastatin acid (4.8-fold), pitavastatin (3.3-fold), atorvastatin (3.2-fold), pravastatin (two-fold), and rosuvastatin (1.6-fold) [14]. Again, it is important to note that inhibition of other critical disposition pathways including CYP3A4 (simvastatin acid, atorvastatin), BCRP (rosuvastatin, atorvastatin, fluvastatin), and OAT3 (pravastatin, rosuvastatin) would exacerbate any DDI due to OATP1B1 if these pathways were also impacted by the perpetrator drug [14]. In contrast to the statins, inhibition of OATP1B1 contributes only in part (up to a maximum of approximately twofold based on clinical pharmacogenetic evidence) to the observed DDIs perpetrated by gemfibrozil (and its glucuronide metabolite) or cyclosporine on the victim drug repaglinide. The major underlying mechanism for these compounds can be attributed to inhibition of the critical disposition pathways CYP2C8 or CYP3A4, respectively [16]. By scrutinizing observed clinical DDI pharmacokinetic profiles, the increase in plasma concentrations of orally administered victim substrate drugs of OATP1B1 is a result of increased bioavailability due to a reduced hepatic uptake mediated by the inhibition of the transporter, as evidenced by the absence of a change in time to maximal peak plasma concentration and in the elimination phase slope and half-life of the drug.

OATP1B3

OATP1B3 has been deemed to be important for clinically relevant transporter disposition and DDIs by regulatory authorities and the International Transporter Consortium for substrate drugs such as the statins (pitavastatin and rosuvastatin), telmisartan, and olmesartan [1].

Transporter Drug Interactions, Table 1 Examples of clinically relevant transporter-mediated drug-drug interactions

Transporter	Victim	Perpetrator	Observed AUC increase *(AUC increase due to inhibition of specific transporter if multiple mechanisms combine for DDI[a])*	Other ADME pathways contributing to observed DDI	References
P-gp	Digoxin	Quinidine	1.54-fold	NA	[9]
		Talinolol	1.23-fold	NA	[10]
		AZD5672	1.33-fold	NA	[11]
		Fostamatinib	1.37-fold	NA	[12]
BCRP	Topotecan	Elacridar	2.4-fold	P-gp	[13]
	Rosuvastatin	Cyclosporine	7.1-fold *(1.9-fold)*	OATP1B1/ OATP1B3/ NTCP	[14]
		Fostamatinib	1.96-fold	NA	[15]
		Eltrombopag	1.88-fold	NA	[15]
		Darunavir	1.48-fold	NA	[15]
		Lopinavir	2.1-fold *(1.7-fold)*	OATP1B1	[15]
		Clopidogrel	1.96-fold *(1.7-fold)*	OATP1B1	[15]
		Ezetimibe	1.21-fold	NA	[15]
		Fenofibrate	1.07-fold	NA	[15]
	Fluvastatin	Cyclosporine	1.9-fold	NA	[14]
OATP1B1	Simvastatin acid	Gemfibrozil	2.85-fold	NA	[14]
		Cyclosporine	8-fold *(4.4-fold)*	CYP3A4	[14]
	Atorvastatin	Cyclosporine	8.7-fold *(3.2-fold)*	BCRP/ CYP3A4	[14]
	Rosuvastatin	Cyclosporine	7.1-fold *(1.6-fold)*	BCRP/ OATP1B3/ NTCP	[14]
		Gemfibrozil	1.9-fold *(1.5-fold)*	OAT3/ OATP1B3	[14]
	Pravastatin	Cyclosporine	3.82-fold *(2.0-fold)*	MRP2	[14]
		Gemfibrozil	2-fold *(1.6-fold)*	OAT3	[14]
	Pitavastatin	Cyclosporine	4.55-fold	NA	[14]
	Repaglinide	Gemfibrozil	8.1-fold *(~2-fold based on PGx)*	CYP2C8	[23]
		Cyclosporine	2.5-fold	CYP3A4	[23]
OAT1/ OAT3	Adefovir	Probenecid	2.09-fold		[24]
	Furosemide	Probenecid	2.68-fold		[24]
	Ciprofloxacin	Probenecid	1.72-fold		[25]
OCT2	Metformin	Dolutegravir	1.79-fold		[24]
	Dofetilide	Cimetidine	1.48-fold	MATE1/ MATE2-K?	[26]
	Pindolol	Cimetidine	1.38–1.47-fold	MATE1/ MATE2-K?	[27]
MATE1/ MATE2-K	Metformin	Cimetidine	1.46–1.54-fold		[19]
		Trimethoprim	1.30–1.37-fold		[19]
		Pyrimethamine	1.39-fold		[19]
	Procainamide	Cimetidine	1.35-fold		[28]
	Varenicline	Cimetidine	1.29-fold		[29]
	Pilsicainide	Cimetidine	1.33-fold		[30]
OCT1	Fenoterol	?	~2-fold *(based on PGx evidence)*		[8]

[a]Derived from mechanistic static equation AUCR predictions

Yet, despite this fact, it is hard to find a reported clinical DDI that can be solely attributed to inhibition of OATP1B3, which likely reflects the very minor contribution OATP1B3 plays towards the overall hepatic elimination of some of these listed substrates. Indeed, OATP1B3 transport only accounts for 10% ($f_e = 0.08$) or 16% ($f_e = 0.11$) of the overall active hepatic elimination of pitavastatin or rosuvastatin, respectively, with the remaining fraction of active uptake being predominantly mediated by OATP1B1 [14]. Therefore, it is actually OATP1B1 (not OATP1B3) that is responsible for driving the ensuing increase in these victim drug exposures when inhibited in DDI, and OATP1B3 simply contributes a very small increase ($\leq$ 1.12-fold if completely inhibited) which would be within pharmacokinetic bioequivalence.

OCT1

The International Transporter Consortium has identified inhibition of OCT1 during DDI to potentially be a clinically relevant transporter pathway for the beta-agonist fenoterol (administered via the inhaled route for treating asthma or the intravenous route for suppressing premature labor in pregnancy), from which the ensuing increased plasma levels of the drug might result in cardiovascular side effects in patients [17]. While there is no reported evidence to date of a clinical pharmacokinetic DDI for fenoterol mediated by an inhibitor of this transporter, the recommendation has arisen as a direct consequence of reported clinical pharmacogenetic studies. In these studies, subjects with almost zero function OCT1 phenotype (*OCT1*3*, *OCT1*4*) exhibited a 1.92-fold increase in plasma concentrations (based on exposure; AUC) of intravenously administered fenoterol compared to subjects with normal OCT1 function [8]. By examining the observed clinical pharmacokinetic profiles between OCT1 pharmacogenetic phenotypes, the increase in plasma concentrations of fenoterol in the zero transporter function phenotype is a direct result of decreased hepatic elimination due to the absence of OCT1-mediated hepatic uptake [8]. On the assumption that the OCT1 phenotype described above is almost a complete loss of OCT1 transporter function, then one might expect the same approximately twofold increase in fenoterol exposure as a theoretical maximum AUC increase were OCT1 to be completely inhibited by a perpetrator drug in DDI.

Renal Transporter-Mediated Interactions

OAT1 and OAT3

Clinically significant DDIs attributed to inhibition of OAT1- and/or OAT3-mediated transport are described in Table 1 and typically involve low-permeability, negatively charged (anions) substrate drugs for whom renal elimination is a major disposition pathway that incorporates extensive active renal tubular secretion, as evidenced by their renal clearance being significantly greater than 1.5 times unbound passive filtration clearance. The main perpetrator drug causing renal DDI through the inhibition of OAT-mediated transport is the antidiuretic probenecid. This is unsurprising given its historical use in the Second World War to purposefully decrease the urinary elimination of penicillin in order to increase its plasma concentrations and, as a direct result, allowing lower doses to be used for therapeutic effect, thereby extending limited supplies of the valuable antibiotic [18]. The observed clinical DDIs between probenecid and either of the victim drugs adefovir, furosemide, or ciprofloxacin, perpetrated through its inhibition of OAT-mediated active uptake from blood into renal proximal tubule cells, results in a reduction in measured renal clearance giving approximately a twofold increase in the victim drug's exposure (AUC). This increase is a direct consequence of subsequently elevated plasma concentrations during the elimination phase of the pharmacokinetic profile; evidenced by the shallowing of the elimination slope and an increase in the half-life of the drug, without a significant change in its maximum plasma concentration.

OCT2, MATE1, and MATE2-K

Clinically significant DDIs attributed to inhibition of OCT2-, MATE1-, and/or MATE2-K-mediated transport are described in Table 1.

These typically involve low-permeability, positively charged (cations) substrate drugs for whom renal elimination is a major disposition pathway. Extensive active renal tubular secretion is often implicated, as evidenced by their renal clearance being significantly greater than 1.5 times unbound passive filtration clearance. The most common perpetrator drug causing renal DDI through inhibition of cation transporters is the gastric acid reducer cimetidine. Similarly to the OAT DDIs above, from a basolateral uptake transporter perspective inhibition of OCT2 uptake, as the mechanism underpinning DDI, results in a reduced renal clearance of the victim drug (e.g., dofetilide and pindolol), yielding elevated plasma concentrations and up to a 1.5-fold increase in AUC in addition to an increase in elimination half-life of the drug.

However, in some instances the same perpetrator drug cimetidine might drive a DDI through a mechanism other than inhibition of OCT2, namely, through a more potent inhibition of MATE1 and/or MATE2-K efflux transporters, depending on the victim substrate drug in question. This mechanism is believed to behind the DDIs perpetrated by cimetidine with procainamide, varenicline, or pilsicainide and results in a similar change to each victim drug's pharmacokinetic profile due to decreased renal clearance by cimetidine, accompanied by subsequent increased plasma concentrations (typically less than a 1.5-fold increase in AUC) and elimination half-life. Typically, for poorly permeable and charged substrate drugs that require secondary active uptake transporters to enter renal proximal tubule cells, inhibition of an apically located efflux transporter (such as MATE) involved in its elimination into urine would not be expected to result in a change in systemic blood concentrations. Rather, inhibition of efflux would be anticipated to increase intracellular concentrations of the substrate drug within the renal cell, without impacting blood levels. However, this is not the case for drugs that are substrates of both OCT2 on the basolateral membrane and MATE1/2-K on the apical membrane. For these compounds, inhibition of MATE, in the absence of OCT2 inhibition, results in elevated blood concentrations of the victim substrate drug. This observation can be explained by the fact that OCT2 is a passive facilitative transporter that aids the movement of a substrate (e.g., procainamide, varenicline, or pilsicainide) down its passive concentration gradient. As such, when MATE is inhibited, thereby preventing elimination into urine, intracellular concentrations of the substrate increase resulting in a rapid shallowing (towards equilibrium) of the inwardly directed concentration gradient from blood, consequently slowing the rate of uptake transport by OCT2 into the proximal tubule cell. The knock-on effect of this indirect reduction in OCT2 function becomes elevated blood concentration as less drug is renally cleared from the systemic circulation.

The most common clinically relevant victim co-medication drug susceptible to reduced renal clearance in DDI through inhibition of either OCT2 or MATE is the antidiabetic metformin. However, while the inhibition of OCT2 is the mechanism through which dolutegravir perpetrates DDI with metformin, the predominant underlying mechanism behind the majority of the clinically observed DDIs with perpetrators, such as cimetidine, trimethoprim, and pyrimethamine, is in fact inhibition of MATE1. These drugs exhibit significantly more potent inhibitory potential against MATE1 versus OCT2 (MATE1 inhibition constant (K_i) values being 35- to 170-fold lower than corresponding OCT2 K_i values, depending on the perpetrator) [19]. For dolutegravir, with respect to its inhibitory properties, the reverse scenario is true and hence explains why inhibition of OCT2 drives its DDI. Regardless of the mechanism, the decrease in metformin renal clearance through cation transporter inhibition results in elevated plasma concentrations and exposure (AUC) of metformin. However, due to the unusual "flip-flop" pharmacokinetic properties exhibited by metformin, these changes are not reflected as a typical AUC profile change on elimination phase, as described above for other renal DDIs, rather it appears as an effect on the "absorptive" phase of the profile, which for metformin actually represents its renal elimination [19].

In Vitro Determination of Transporter Interaction Potential

Studying transporter interaction potential in vitro typically utilizes test systems of either immortalized cell lines such as intestinal-derived Caco-2 (for BCRP) or transfected cell lines such as Madin-Darby canine kidney (MDCK) or human embryonic kidney 293 (HEK293) overexpressing a human transporter gene (e.g., MDR1 in MDCK cells for P-gp or an SLC transporter in HEK293 cells). Polarized Caco-2 or MDCK-MDR1 cell monolayers on membrane inserts are used as the gold standard to assess interactions with BCRP or P-gp efflux transporters, respectively, as these cells differentiate into a brush border-type membrane barrier complete with tight junctions similar to physiological barriers, allowing measurement of flux across the barrier (please see accompanying chapter ▶ "Drug Permeability and Transporter Assessment: Polarized Cell Lines" for more detail of the methodology). For studying SLC uptake transporters, transfected HEK293 cells are used as plated monolayers, and measurement into cells is determined and compared to mock vector control cells (please see accompanying chapter ▶ "Drug Transport Assessment: Transfected Cells and Membrane Vesicles" for more detail of the methodology).

Inhibitor (Perpetrator) Liability

During drug development, in order to evaluate the in vitro inhibitory potential of an investigational drug against a particular transporter, the transport of a clinically relevant probe substrate (or demonstrated surrogate) of that transporter is measured in one of the appropriate cell test systems described above. Studies are conducted in the absence (termed the vehicle control) and in the presence of increasing concentrations of the investigational drug (e.g., 0.3, 1, 3, 10, 30, and 100 μM). The uninhibited transport activity determined in the vehicle control condition is assigned 100% transport activity, and all transport activities determined in the presence of investigational drug are converted to percentages of this control transport activity. These are subsequently plotted against nominal inhibitor concentration and fitted, typically using a four-parameter logistical equation, in order to determine the inhibitory concentration value that inhibits transport activity to 50% (IC_{50}) [11, 15, 19]. For transporter inhibition assessment, it is industry-wide standard practice to use a probe substrate concentration that is much lower (five to ten times) than its transport affinity constant (Michaelis-Menten kinetic constant, K_m) for the transporter so that the determined IC_{50} value is equivalent to the absolute inhibition constant K_i, assuming inhibition is competitive [20]. Furthermore, in order to ensure that the correct value for IC_{50} is obtained during the in vitro studies, it is imperative that all inhibition assessments, regardless of the transporter, include a preincubation step with the investigational drug (of sufficient duration to allow time for entry of the drug inside the cell). This should potentially avoid underestimating the IC_{50} value, which would occur if a preincubation was not performed and the investigational drug needed to exert an additional effect at an intracellular site of the transporter as part of its mechanism of inhibition [21]. This artefactual in vitro phenomenon is particularly an issue when using HEK-293 SLC transporter-expressing cell systems for transporter inhibition assessments as these commonly utilize very short incubation times (< 5 minutes) which may, depending on the specific investigational drugs physicochemical properties and associated passive diffusive permeability, impede the occurrence of any intracellular effect.

Substrate (Victim) Liability

During the regulatory development of a drug, in order to evaluate the in vitro substrate potential for a particular transporter, the bidirectional apparent permeability, or uptake, of a range of concentrations of the investigational drug (spanning a 100-fold range; typically, 1, 10, 50, and 100 μM) is determined in one of the appropriate cell test systems described above for ABC efflux transporters (P-gp, BCRP) or uptake transporters (SLCs), respectively. For ABC efflux transporters, a comparison of bidirectional permeability values is used to calculate an efflux ratio (see chapter ▶ "Drug Permeability and Transporter

Assessment: Polarized Cell Lines"), whereas for SLC uptake transporters, the uptake rate determined in transporter-transfected cells is compared to that determined in the corresponding vector control transfected cells in order to calculate an uptake ratio (see chapter ▶ "Drug Transport Assessment: Transfected Cells and Membrane Vesicles"). Based on current regulatory DDI guidance, an investigational drug is classified as a substrate of a transporter if its efflux/uptake ratio determined at a low (non-saturating) test concentration is >2 and inhibited by over 50% in the presence of a known reference inhibitor for the transporter in question. It is important to note that if an investigational drug has high intrinsic passive membrane permeability, then transporters are unlikely to play a major role in its disposition within the body, and as such transporter substrate assessment is not required by regulators. This assessment of permeability on ADME can be determined using the framework set out in the Biopharmaceutics Classification System which directs that BCS class 1 compounds with high permeability are unlikely to be impacted by transporters, whereas class 3 and 4 compounds with low permeability are likely to be impacted by transporters.

Assessing DDI Risk

It is quite difficult to assess "victim" DDI risk for an investigational drug that has been shown to be a substrate of transporters as several factors need to be taken into consideration. These include its concentration at the interacting site, what the percentage of active transport versus passive diffusion is to derive the fraction excreted value assigned to the transporter, and whether it contributes to a critical ADME pathway for the drug (>25% overall clearance; often not known until the human radiolabeled mass balance study is conducted in Phase 2b clinical trials). All this knowledge then has to be contextualized with its anticipated therapeutic window (safety margin) to understand the risk should there be an increase in its exposure through DDI.

In contrast, it is common practice in late drug discovery and in early drug development before clinical studies in patients, to assess the risk of an investigational drug perpetrating a DDI through inhibition of transporters at its expected therapeutic dose. For orally administered drugs, the risk is determined using basic static equations. The anticipated inhibitor concentration at the transporter interaction site (corresponding to theoretical intestinal luminal concentration, unbound hepatic inlet concentration, or unbound maximum plasma concentration at steady state; for intestinal efflux transporters [P-gp or BCRP], hepatic uptake transporters [OATP1B1, OATP1B3, or OCT1] or renal transporters [OAT1, OAT3, OCT2, MATE1 or MATE2-K], respectively) is divided by the K_i value for inhibition in order to calculate a ratio. If this numerical value exceeds the predetermined ratio thresholds (cut-offs) as stipulated by the various regulatory authority DDI guidance, then the investigational drug is considered to have the potential to cause a *qualitative* DDI in the clinic and, as such, would need to be considered for further investigation in a follow-up clinical DDI study with a sensitive clinical probe substrate (victim) to confirm if it is indeed a transporter inhibitor in vivo. Both the in vitro transporter inhibition data and any subsequent clinical DDI data are included on a new drug's label to inform physicians around what common co-medications can/cannot be co-administered safely during clinical use with the drug.

Quantitative Prediction of Transporter and Complex DDIs

The problem with the *qualitative* in vitro DDI risk assessment above is that it is an "all or nothing" approach that simply flags DDI potential and might lead to physicians excluding vulnerable victim co-medications from clinical trials for reasons of patient safety. This can then have a major impact on patient recruitment to such studies if a patient could not be taken off that co-medication.

An alternative more valuable approach, using generated in vitro inhibitory data with mechanistic static equations, is to consider the *quantitative* prediction of DDI liability in order to forecast the exposure (AUC) increase of a common victim co-medication due to inhibition of transporter

pathways by a perpetrator drug. Such an approach provides context to physicians who, using their knowledge around the therapeutic index of the victim co-medication, can make an informed decision on whether any potential DDI is simply a pharmacokinetic DDI or more importantly a clinically significant DDI requiring clinical intervention (e.g., monitoring, dose adjustment, or contraindication of the co-medication). Mechanistic static equations require knowledge of the critical disposition pathways of the victim drug and use the ratio of inhibitor concentration divided by K_i within the context of the derived fraction excreted (f_e) value for the transporter pathway to predict maximal theoretical fold change in AUC one might expect if that pathway was inhibited in DDI (see the review of Elsby et al. [14] for more detail). Such predictions represent the "worst-case" scenario and assume that the victim and perpetrator drugs are at the interaction site at the same time and at maximal concentrations. Successful quantitative prediction of transporter-mediated DDIs (where predictions matched the clinically observed fold increase in AUC) has been used to confirm that the mechanisms underpinning DDIs with metformin [19] or rosuvastatin [15] are due to inhibition of MATE1 or intestinal BCRP, respectively (see Table 1).

For a large number of victim co-medications, more complex DDIs can occur and can exacerbate the transporter-mediated impact if the victim drug's principal ADME pathways also involve metabolizing enzymes that are equally susceptible to inhibition by the same perpetrator drug clinically. Statins are examples of drugs that are susceptible to complex DDIs, and this is a regulatory concern due to the prevalence of statin prescriptions in many disease areas due to comorbidities, thus making them a common co-medication for which the potential for DDI is high [7]. Quantitative DDI prediction using mechanistic static equations has been utilized to determine the individual contribution each specific ADME pathway plays when inhibited towards the overall clinically observed statin DDI (as highlighted in Table 1). From such analysis, it is apparent for simvastatin acid and atorvastatin that inhibition of hepatic OATP1B1 is responsible for approximately 50% of the observed fold increase in AUC in DDI with cyclosporine, with the remaining exposure increases being attributed to reversible inhibition of both intestinal and hepatic cytochrome P450 3A4 [14]. However, if a perpetrator drug is predicted to be a relatively weak inhibitor of OATP1B1 with these two statins but a clinical time-dependent inhibitor (inactivator) of cytochrome P450 3A4, as well as potentially a reversible inhibitor, then the causative balance of overall DDI magnitude could shift entirely towards inhibition of the drug-metabolizing enzyme as the sole driving force of the observed DDI. This is the case for the reported DDIs between simvastatin acid and telithromycin or clarithromycin, where a 9.3-fold increase (observed 10.7-fold) or 8.4-fold increase (observed 11.6-fold) in AUC, respectively, are predicted to result from inhibition and inactivation of intestinal and hepatic cytochrome P450 3A4 alone, with minimal impact from OATP1B1 [22].

In the future, given the value of the approach towards delineating complex DDIs, it is conceivable that quantitative DDI predictions could be included, alongside in vitro transporter inhibition data, in drug labels to inform prescribers around patient safety with respect to the DDI risk with co-medications.

Cross-References

- ▶ Drug Permeability and Transporter Assessment: Polarized Cell Lines
- ▶ Drug Transport Assessment: Transfected Cells and Membrane Vesicles

References

1. Giacomini KM, Huang S-M, Tweedie DJ, Benet LZ, Brouwer KLR, Chu X, et al. Membrane transporters in drug development. Nat Rev Drug Discov. 2010;9:215–36.
2. Lee CA, O'Connor MA, Ritchie TK, Galetin A, Cook JA, Ragueneau-Majlessi I, et al. Breast cancer resistance protein (ABCG2) in clinical pharmacokinetics and drug interactions: practical recommendations for clinical victim and perpetrator drug-drug interaction study design. Drug Metab Dispos. 2015;43:490–509.

3. Giacomini KM, Balimane PV, Cho SK, Eadon M, Edeki T, Hillgren KM, et al. International Transporter Consortium commentary on clinically important transporter polymorphisms. Clin Pharmacol Ther. 2013;94:23–6.
4. Birmingham BK, Bujac SR, Elsby R, Azumaya CT, Wei C, Chen Y, et al. Impact of ABCG2 and SLCO1B1 polymorphisms on pharmacokinetics of rosuvastatin, atorvastatin and simvastatin acid in Caucasian and Asian subjects: a class effect? Eur J Clin Pharmacol. 2015;71:341–55.
5. Wu HF, Hristeva N, Chang J, Liang X, Li R, Frassetto L, Benet LZ. Rosuvastatin pharmacokinetics in Asian and White subjects wild-type for both OATP1B1 and BCRP under control and inhibited conditions. J Pharm Sci. 2017;106:2751–7.
6. Pizzagalli MD, Bensimon A, Superti-Furga G. A guide to plasma membrane solute carrier proteins. FEBS J. 2020; https://doi.org/10.1111/febs.15531. Online ahead of print.
7. Williamson B, Riley R. Hepatic transporter drug-drug interactions: an evaluation of approaches and methodologies. Expert Opin Drug Metab Toxicol. 2017;13:1237–50.
8. Tzvetkov MV, Matthaei J, Pojar S, Faltraco F, Vogler S, Prukop T, et al. Increased systemic exposure and stronger cardiovascular and metabolic adverse reactions to fenoterol in individuals with heritable OCT1 deficiency. Clin Pharmacol Ther. 2018;103:868–78.
9. Pedersen KE, Christiansen BD, Klitgaard NA, Nielsen-Kudsk F. Effect of quinidine on digoxin bioavailability. Eur J Clin Pharmacol. 1983;24:41–7.
10. Westphal K, Weinbrenner A, Giessmann T, Stuhr M, Franke G, Zschiesche M, et al. Oral bioavailability of digoxin is enhanced by talinolol: evidence for involvement of intestinal P-glycoprotein. Clin Pharmacol Ther. 2000;68:6–12.
11. Elsby R, Gillen M, Butter C, Imisson G, Sharma P, Smith V, et al. The utility of in vitro data in making accurate predictions of human P-glycoprotein mediated drug-drug interactions: a case study for AZD5672. Drug Metab Dispos. 2011;39:275–82.
12. Martin P, Gillen M, Millson D, Oliver S, Brealey C, Elsby R, et al. Effects of fostamatinib on the pharmacokinetics of digoxin (a P-glycoprotein substrate): results from in vitro and Phase I clinical studies. Clin Ther. 2015;37:2811–22.
13. Kruijtzer CMF, Beijnen JH, Rosing H, ten Bokkel Huinink WW, Schot M, Jewell RC, et al. Increased oral bioavailability of topotecan in combination with the breast cancer resistance protein and P-glycoprotein inhibitor GF120918. J Clin Oncol. 2002;20:2943–50.
14. Elsby R, Hilgendorf C, Fenner K. Understanding the critical disposition pathways of statins to assess drug-drug interaction risk during drug development: it's not just about OATP1B1. Clin Pharmacol Ther. 2012;92:584–98.
15. Elsby R, Martin PD, Surry D, Sharma P, Fenner K. Solitary inhibition of the breast cancer resistance protein (BCRP) efflux transporter results in a clinically significant drug-drug interaction with rosuvastatin by causing up to a two-fold increase in statin exposure. Drug Metab Dispos. 2016;44:398–408.
16. Prandin® (repaglinide) US FDA drug label (Ref ID 4052550) (2009) Novo Nordisk. Accessed via Drugs@FDA database. www.accessdata.fda.gov/scripts/cder/daf/.
17. Chu X, Liao M, Shen H, Yoshida K, Zur AA, Arya V, et al. Clinical probes and endogenous biomarkers as substrates for transporter drug-drug interaction evaluation: perspectives from the International Transporter Consortium. Clin Pharmacol Ther. 2018;104:836–64.
18. Landersdorfer CB, Kirkpatrick CM, Kinzig M, Bulitta JB, Holzgrabe U, Jaehde U, et al. Competitive inhibition of renal tubular secretion of ciprofloxacin and metabolite by probenecid. Br J Clin Pharmacol. 2010;69:167–78.
19. Abel S, Nichols DJ, Brearley CJ, Eve MD. Effect of cimetidine and ranitidine on pharmacokinetics and pharmacodynamics of a single dose of dofetilide. Br J Clin Pharmacol. 2000;49:64–71.
20. Somogyi AA, Bochner F, Sallustio BC. Stereoselective inhibition of pindolol renal clearance by cimetidine in humans. Clin Pharmacol Ther. 1992;51:379–87.
21. Somogyi A, McLean A, Heinzow B. Cimetidine-procainamide pharmacokinetic interaction in man: evidence of competition for tubular secretion of basic drugs. Eur J Clin Pharmacol. 1983;25:339–45.
22. Feng B, Obach RS, Burstein AH, Clark DJ, de Morais SM, Faessel HM. Effect of human renal cationic transporter inhibition on the pharmacokinetics of varenicline, a new therapy for smoking cessation: an in vitro-in vivo study. Clin Pharmacol Ther. 2008;83:567–76.
23. Shiga T, Hashiguchi M, Urae A, Kasanuki H, Rikihisa T. Effect of cimetidine and probenecid on pilsicainide renal clearance in humans. Clin Pharmacol Ther. 2000;67:222–8.
24. Varma MV, Lai Y, Kimoto E, Goosen TC, El-Kattan AF, Kumar V. Mechanistic modeling to predict the transporter- and enzyme-mediated drug-drug interactions of repaglinide. Pharm Res. 2013;30:1188–99.
25. Zamek-Gliszczynski MJ, Giacomini KM, Zhang L. Emerging clinical importance of hepatic organic cation transporter 1 (OCT1) in drug pharmacokinetics, dynamics, pharmacogenetic variability, and drug interactions. Clin Pharmacol Ther. 2018;103:758–60.
26. Robbins N, Koch SE, Tranter M, Rubinstein J. The history and future of probenecid. Cardiovasc Toxicol. 2012;12:1–9.
27. Elsby R, Chidlaw S, Outteridge S, Pickering S, Radcliffe A, Sullivan R, et al. Mechanistic in vitro studies confirm that inhibition of the renal apical efflux transporter multidrug and toxin extrusion (MATE) 1, and not altered absorption, underlies the increased metformin exposure observed in clinical interactions with cimetidine, trimethoprim or pyrimethamine. Pharmacol Res Perspect. 2017;5:e00357.

28. Cheng Y, Prusoff WH. Relationship between the inhibition constant (K_i) and the concentration of inhibitor which causes 50 per cent inhibition (I_{50}) of an enzymatic reaction. Biochem Pharmacol. 1973;22:3099–108.
29. Tátrai P, Schweigler P, Poller B, Domange N, de Wilde R, Hanna I, et al. A systematic in vitro investigation of the inhibitor preincubation effect on multiple classes of clinically relevant transporters. Drug Metab Dispos. 2019;47:768–78.
30. Elsby R, Hare V, Neal H, Outteridge S, Pearson C, Plant K, et al. Mechanistic in vitro studies indicate that the clinical drug-drug interaction between telithromycin and simvastatin acid is driven by time-dependent inhibition of CYP3A4 with minimal effect on OATP1B1. Drug Metab Dispos. 2019;47:1–8.

Two-Compartment Pharmacokinetic Model

Alan Talevi[1,2] and Carolina L. Bellera[1,3]
[1]Laboratory of Bioactive Research and Development (LIDeB), Department of Biological Sciences, University of La Plata (UNLP), La Plata, Buenos Aires, Argentina
[2]Argentinean National Council of Scientific and Technical Research (CONICET) – CCT, La Plata, Buenos Aires, Argentina
[3]Consejo Nacional de Investigaciones Científicas y Técnicas (CONICET), La Plata, Buenos Aires, Argentina

Definition

The two-compartment pharmacokinetic model describes the evolution of drug levels in the organism by depicting the body as two pharmacokinetic compartments (the central and the peripheral compartments, also commonly referred to as compartment 1 and compartment 2, in that order). Once a given drug amount reaches one of these compartments, it distributes throughout it immediately and homogenously. However, movement from one compartment to the other is not instantaneous but follows first-order kinetics. As in the one-compartment model, drug elimination occurs following (apparent) first-order kinetics. By default (i.e., unless otherwise specified), it is assumed that elimination occurs only from the central compartment (Fig. 1). Depending on the modelled therapeutic scenario, drug absorption will be assumed to be instantaneous (e.g., intravenous bolus) or to follow zero- or first-order kinetics (e.g., constant-rate intravenous infusion or extravascular drug administration, respectively). It is also assumed that the drug initially enters the central compartment, from which it distributes to the peripheral one. Two-compartment models are the most common in population pharmacokinetic modeling: it has been estimated that they represent around 80% of published models [1, 2]. By integrating the mass balances for each compartment, it is possible to obtain equations of drug amount in each compartment versus time *t*.

Generalities and Assumptions

Pharmacokinetic models are derived by writing and solving the correspondent mass balance equations. In compartmental analysis, one mass balance equation is considered for each compartment represented in the model. In the two-compartment model, two mass balance equations will be required at first (a third compartment can eventually be depicted to explicitly consider the absorption site). Mass balance equations obey the following general form:

$$\frac{dA_i}{dt} = [rate\ of\ drug\ in] - [rate\ of\ drug\ out] \quad (1)$$

where dA_i/dt denotes the instantaneous rate of change of the amount of drug in the compartment i and the terms on the right denote the difference between the rates at which drug molecules enter and exit such compartment. Conventionally (but understandably), the terms that represent the rate at which the drug enters the compartment are positive, as they represent drug gain, whereas the terms that represent drug loss for the compartment are negative.

Neither the central compartment nor the peripheral compartment has an immediate anatomical or physiological meaning. They are, in

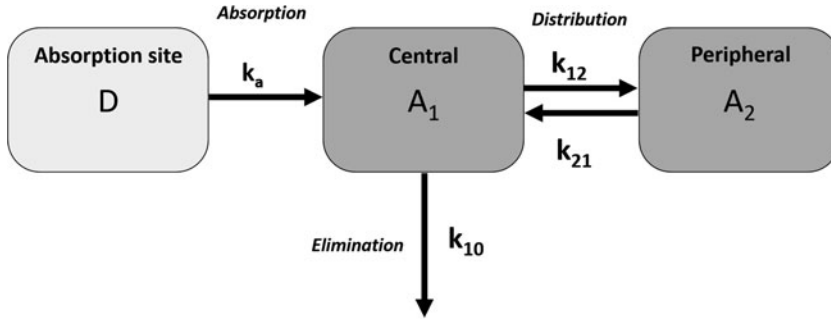

Two-Compartment Pharmacokinetic Model, Fig. 1 Schematic representation of the two-compartment model. Here, first-order absorption of a dose D from the absorption site (with kinetic constant k_a) is shown. However, depending on the chosen route (and way) of drug administration, it might be assumed that the drug enters the compartment instantaneously (e.g., intravenous bolus) or following zero-order kinetics (e.g., intravenous infusion at constant rate). D is the dose, and A_1 and A_2 represent the (time-dependent) amounts of drug in the central and peripheral compartments, respectively. k_a, k_{12}, k_{21}, and k_{10} denote the so-called micro-constants: the first-order kinetic rate constants for absorption, distribution, redistribution, and elimination, in that order

principle, only mathematical constructs, abstractions. However, it can be reasonably assumed that the central compartment condenses the intravascular space plus all the well-irrigated organs for which mass exchange with blood is favored (for instance, lungs, liver, and kidneys), thus rapidly equilibrating with blood. On the other hand, the peripheral compartment condenses those organs or tissues that equilibrate with blood in a slow manner, e.g., poorly irrigated tissues or organs like bones, skin, and adipose tissue. Under this light, it is sensible to consider that elimination takes places exclusively from the central compartment, as the main drug eliminating organs are associated to it.

The assumption that drug elimination follows apparent linear elimination kinetics (in other words, the rate of elimination is assumed to be proportional to the amount of drug remaining in the compartment) is also a reasonable approximation in most therapeutic situations, as often the free drug concentration for most drugs in biological fluids is below the Michaelis-Menten Km value of those saturable systems (transporters, enzymes) involved in the elimination process. On the other hand, it is realistic to assume that distribution from compartment 1 to compartment 2 and redistribution from compartment 2 to compartment 1 follow (apparent) first-order kinetics. First, free diffusion is the most common mechanism of drug permeation across biological barriers, and it is indeed a linear, non-saturable process. Second, as already mentioned, therapeutic agents rarely reach free levels that saturate transport systems. Below saturation conditions, Michaelean kinetics can be approximated to first-order kinetics.

Intravenous Bolus

For the sake of simplicity, the intravenous administration of a drug (intravenous bolus) will be considered in the first place. For all practical purposes, the dose D is delivered rapidly and directly into the central compartment (where systemic circulation lies) by an injection over a (very) short time period. Intravenous injection can thus be regarded as a case of instantaneous absorption process. Since drug administration occurs from the central compartment, the mass balance for compartment 1 can be written as follows:

$$\frac{dA_1}{dt} = -k_{10}\,A_1 - k_{12}A_1 + k_{21}A_2 \qquad (2)$$

where k_{10} represents the elimination rate constant and k_{12} and k_{21} denote the kinetic constants associated to the movement of the drug from the central to the peripheral compartment and vice

versa, respectively. The movement of drug molecules from compartment 1 to compartment 2 is sometimes referred as *distribution*, whereas the inverse movement from compartment 2 to compartment 1 is sometimes referred as *redistribution*. A_1 denotes the amount of drug in the central compartment which is, of course, time-dependent.

The mass balance for compartment 2, in the other hand, takes the following form:

$$\frac{dA_2}{dt} = k_{12}A_1 - k_{21}A_2 \qquad (3)$$

A_2 denotes the amount of drug in the peripheral compartment which is also time-dependent. Note that, at any time point after administration (until the dose has been completely removed from the system), drug molecules will be flowing in both directions, from compartment 1 to compartment 2 and vice versa. However, depending on the specific moment/phase, drug movement in one sense will predominate over drug movement in the other one.

Right after injection of the dose D (i.e., time $t \approx 0$), the amount of drug in the peripheral compartment is negligible, as practically the whole dose is located within compartment 1, and drug distribution from the central to the peripheral compartment has just started. Accordingly, the positive redistribution term in Eq. 2 is much smaller than the negative terms. The instantaneous rate at which A_1 changes is negative (< 0), and it depends on the contributions of both the distribution and elimination processes. This initial phase of the correspondent concentration versus time profile in the central compartment is also termed *fast disposition (distribution plus elimination) phase* or *α-phase*, as there is a net flow of molecules from compartment 1 to compartment 2 and from compartment 1 to the exterior of the system as well [Eq. (2)]. This is also evident from Eq. (3), as immediately after administration of the drug, the redistribution term would be small (as there is practically no drug in the peripheral compartment), while the distribution term is large, since virtually all the dose is still in the central compartment. Therefore, the instantaneous rate at which the amount of drug in the peripheral compartment changes, dA_2/dt, will be > 0 during the fast disposition phase, which indicates that in this phase the amount of drug in compartment 2 is rising (Fig. 2).

Eventually, though, as the amount of drug in the central compartment is falling while the

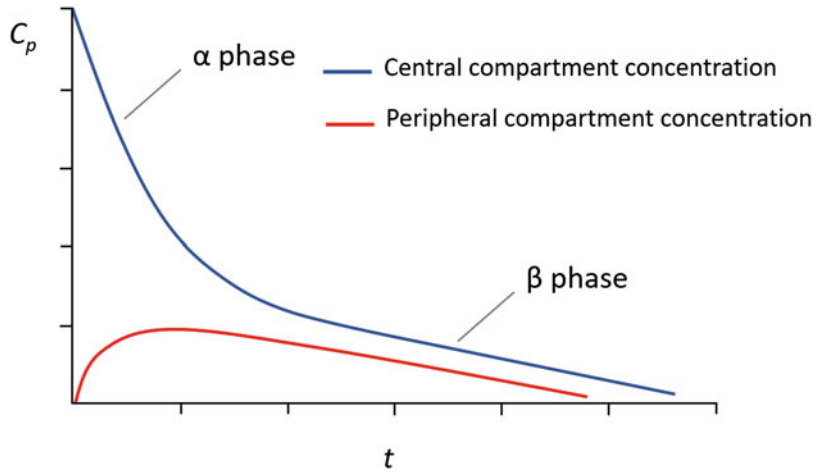

Two-Compartment Pharmacokinetic Model, Fig. 2 Evolution of drug concentrations in the central and peripheral compartments over time. Initially, drug distribution and elimination from the central compartment predominate, which explains the rapid decay of drug concentration in compartment 1 during the α-phase. Eventually, both compartments (transiently) equilibrate (steady state), and a moment later the terminal or *β*-phase begins. It is characterized by the elimination of drug from the body, once central and peripheral compartments collapse to a one-compartment model. In this last phase, the drug levels in both compartments evolve in parallel

amount in the peripheral compartment is increasing, the product ($k_{12} \cdot A_1$) will be equal in magnitude to ($k_{21} \cdot A_2$), and the distribution and redistribution terms will mutually cancel. In other words, in that moment (and for just a moment), there will be no net exchange of drug between the compartments, i.e., *steady state* has been reached. Note that at steady state Eqs. (2) and (3) take the following form:

$$\left.\frac{dA_1}{dt}\right|_{steady-state} = -k_{10}A_1 \tag{4}$$

$$\left.\frac{dA_2}{dt}\right|_{steady-state} = 0 \tag{5}$$

At that moment, the amount of drug in the body is only influenced by the elimination processes that occur in the central compartment. Immediately after, a concentration gradient is again created, but this time in the opposite direction. This is because of the continual elimination of drug from the central compartment: a moment after steady state, some drug has been eliminated from compartment 1, and then, $(k_{12} \cdot A_1) < (k_{21} \cdot A_2)$. In response to this, drug flows back into the central compartment to follow the decay of drug in it. In fact, this process of "redistribution" (net return of drug from the peripheral to the central compartment) slows down the rate of decay of the drug levels in compartment one. After the steady state, or true equilibrium, the *terminal phase, slow disposition phase*, or *β-phase* begins, which may be viewed as a pseudo equilibrium where the amount of drug in both compartments evolves in parallel (the concentrations in both compartments decrease proportionally). The rather slow decline in drug concentration in the central compartment during this terminal phase is sustained by redistribution of drug from tissue stores.

The volumes of the central (V_1) and peripheral (V_2) compartments relate the amount of drug in each of them with the correspondent concentrations. The concentration of drug in the central compartment is much more easily assessed experimentally than the concentration in the peripheral one (by measuring plasma concentrations).

The relationship between the three micro-rate constants determines the shape of the concentration versus time curve (i.e., the relative duration of each phase and how pronouncedly drug concentration falls in each of them) and depends on the drug [3]. For instance, lidocaine [4] and oxacillin [5] have similar values for all the three rate constants. Certain drugs accumulate rapidly and extensively in tissues, which is evidenced by comparatively large values of k_{12} (versus k_{21} or k_{10}). This is the case, for example, of diazepam [6]. Drugs like ampicillin, in contrast, present a high k_{10} value compared to the values of both k_{12} and k_{21} [7]. Contrarywise, drugs like theophylline [8] display distribution and redistribution rate constants much larger than the elimination one.

The inadequacy of the simpler one-compartment model to describe the pharmacokinetic behavior of a drug can be graphically evidenced by plotting the logarithm of plasma concentration versus *t*. Deviations from linearity in the log transformed plot clearly suggest the need to incorporate more compartments in the model (Fig. 3).

By applying Laplace transform to the differential Eqs. (2) and (3), Eq. (6) can be written for the central compartment:

$$Cp = C_1 e^{-\alpha t} + C_2 e^{-\beta t} \tag{6}$$

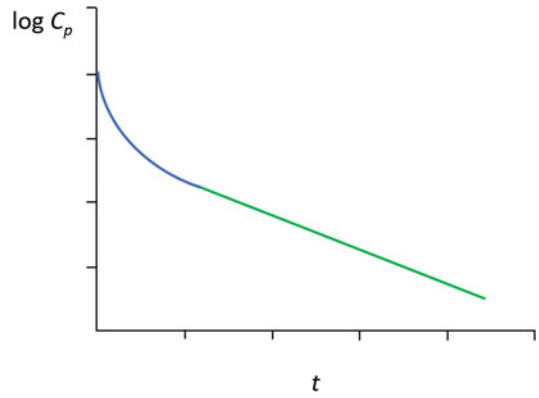

Two-Compartment Pharmacokinetic Model, Fig. 3 Graph of log *Cp* versus *t* for a drug whose pharmacokinetics fits a two-compartment model. The fast disposition phase is shown in blue, whereas the slow disposition phase is shown in green

where α is the overall rate constant associated with the fast disposition phase (sometimes also symbolized λ_1) and β is the overall rate constant associated to the slow disposition phase (sometimes also symbolized λ_2), with α being larger than β. They are referred to as macro-rate (or hybrid) constants, to distinguish them from the previously mentioned micro-rate constants. The micro- and macro-rate constants are connected by Eqs. (7) and (8):

$$\alpha + \beta = k_{12} + k_{21} + k_{10} \tag{7}$$

$$\alpha \cdot \beta = k_{21} \cdot k_{10} \tag{8}$$

Coefficients C_1 and C_2, for their part, are given by Eqs. (9) and (10):

$$C_1 = \frac{Cp_0(\alpha - k_{21})}{\alpha - \beta} \tag{9}$$

$$C_2 = \frac{Cp_0(k_{21} - \beta)}{\alpha - \beta} \tag{10}$$

where Cp_0 denotes the drug concentration in the central compartment at time zero ($dose/V_1$). The equations can be solved by the method of residuals (feathering) which in this case allows to separate fast disposition and slow disposition (similar to the way that is used to estimate the absorption rate constant following extravascular administration for drugs that fit the one-compartment model).

Each phase has its own half-life, which are usually termed fast disposition half-life (Eq. 11) and slow disposition half-life, more often called elimination half-life (Eq. 12):

$$t_{1/2}\big|_{\alpha} = \frac{ln\ 2}{\alpha} \tag{11}$$

$$t_{1/2}\big|_{\beta} = \frac{ln\ 2}{\beta} \tag{12}$$

Usually, the half-life reported by textbooks or drug package inserts (sometimes called the "overall" elimination half-life) corresponds to the half-life for the slowest of the phases, which in general is the elimination phase (see, for instance, refs. [9, 10]) (overall elimination half-life is however frequently estimated through non-compartmental analysis).

As in the one-compartment model, the area under the plasma concentration versus time curve (AUC) is computed as:

$$AUC_0^t = \int_0^t Cp\ dt \tag{13}$$

which, in the framework of the two-compartment model, can be re-written as:

$$AUC_0^t = \int_0^t \left(C_1 e^{-\alpha t} + C_2 e^{-\beta t}\right) dt \tag{14}$$

Integration of the former expression leads to:

$$AUC_0^t = \frac{C_1}{\alpha}\left(1 - e^{-\alpha t}\right) + \frac{C_2}{\beta}\left(1 - e^{-\beta t}\right) \tag{15}$$

If the integration runs from 0 to ∞, that is, if the *total area under the curve* is computed, then:

$$AUC_0^{\infty} = \frac{C_1}{\alpha} + \frac{C_2}{\beta} \tag{16}$$

Replacing C_1 and C_2 by Eqs. (9) and (10), respectively, and after some algebraic manipulation, the following equation is obtained:

$$AUC_0^{\infty} = \frac{Dose}{V_1 \cdot k_{10}} = \frac{Dose}{Clearance} \tag{17}$$

which is the same expression for the total area under the curve for an intravenous bolus in the framework of the one-compartment model.

Intravenous Infusion at Constant Rate

For an intravenous infusion at steady flow rate, the mass balance for the peripheral compartment will not be modified and corresponds to Eq. (3) (note that the drug initially enters the intravascular space, "located" within the central compartment, and from there it distributes to the peripheral

compartment). Contrarywise, the mass balance for the central compartment changes, as it must now incorporate a constant and positive term to account for the zero-order drug input. Equation (2) thus becomes:

$$\frac{dA_1}{dt} = k_0 - k_{10}A_1 - k_{12}A_1 + k_{21}A_2 \qquad (18)$$

where k_0 represents the (constant, i.e., time-independent) infusion rate.

Integration of the system of differential Eqs. (3) and (18) leads to:

$$Cp = \frac{k_0(\alpha - k_{21})}{\alpha\, V_1(\alpha - \beta)}\left(1 - e^{-\alpha t}\right) + \frac{k_0(k_{21} - \beta)}{\beta\, V_1(\alpha - \beta)}\left(1 - e^{-\beta t}\right) \qquad (19)$$

where t is the time measured from the beginning of the intravenous infusion. During the infusion phase, the shape of the concentration-time profile will be similar to that of a drug that fits the one-compartment model. In the post-infusion phase (i.e., after interrupting infusion), the mass balance will be exactly as in Eqs. (2) and (3), and the shape of the concentration-time curve will be identical to the one of an intravenous bolus, that is, two distinctive phases will be observed when log transforming the Cp data (Fig. 4). Succinctly, the plasma concentration will be given by:

$$Cp = \left(C_1 e^{-\alpha t_p} + C_2 e^{-\beta t_p}\right) \qquad (20)$$

where now t_p is the time lapse from the moment the infusion was stopped and C_1 and C_2 depend on how much time the infusion lasted.

$$C_1 = \frac{k_0(\alpha - k_{21})}{\alpha\, V_1(\alpha - \beta)}\left(1 - e^{-\alpha t}\right) \qquad (21)$$

$$C_2 = \frac{k_0(k_{21} - \beta)}{\beta\, V_1(\alpha - \beta)}\left(1 - e^{-\beta t}\right) \qquad (22)$$

Extravascular Administration

Here, the mass balance for the peripheral compartment remains the same (corresponding to Eq. (3)), but the mass balance for the central compartment must include a first-order absorption term:

$$\frac{dA_1}{dt} = k_a\, A_0 - k_{10}A_1 - k_{12}A_1 + k_{21}A_2 \qquad (23)$$

where k_a symbolizes the absorption rate constant (sometimes also denoted k_{01}) and A_0 represents the amount of drug in the absorption site. The following expression represents the mass balance for the absorption site:

$$\frac{dA_0}{dt} = -k_a\, A_0 \qquad (24)$$

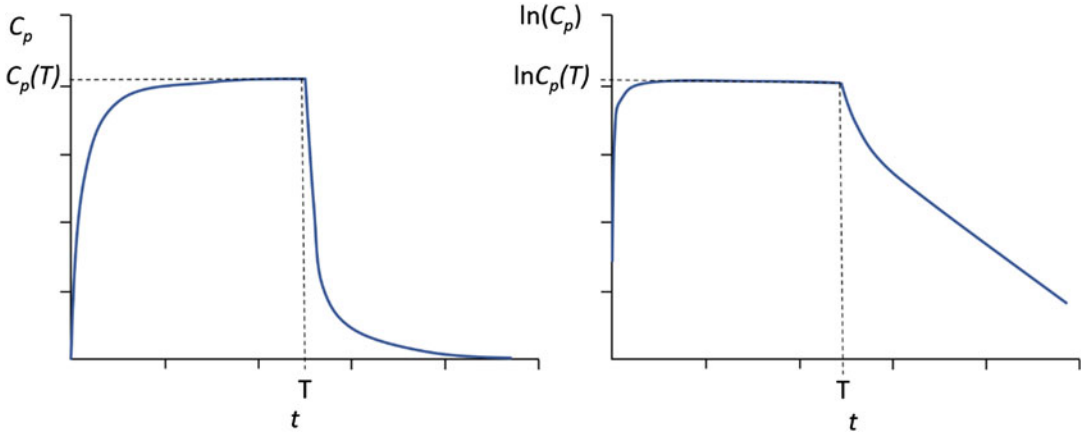

Two-Compartment Pharmacokinetic Model, Fig. 4 Plot of the plasma concentration (Cp) versus t (left) and ln (Cp) versus t (right) for a two-compartment intravenous infusion. T indicates the moment when the infusion is interrupted

which indicates that the amount of drug remaining to be absorbed keeps falling as absorption progresses.

Integrations of the resulting set of Eqs. (3), (23), and (24) provides a rather complex expression of Cp versus t.

$$Cp = \frac{FD}{V_1} k_a \left[\frac{(k_{21} - \alpha)}{(\alpha - k_a)(\alpha - \beta)} e^{-\alpha t} + \frac{(k_{21} - \beta)}{(\beta - k_a)(\beta - \alpha)} e^{-\beta t} + \frac{(k_{21} - k_a)}{(k_a - \alpha)(k_a - \beta)} e^{-k_a t} \right] \tag{25}$$

By calculating the derivative of Cp with respect to t, the time to peak concentration t_{max} can be obtained (by solving t when the derivative equals zero) and, subsequently, the peak concentration.

As can be imagined from the previous equations, compartmental models can be further expanded with an additional compartment (and an additional exponential term!) to account for tissues with distinctive distribution and redistribution kinetics. Naturally, the mathemathics of the resulting equations (and solving the model parameters) will get progressively complicated. The two-compartment model provides a reasonable balance between relatively simple mathematics and applicability.

Volumes of Distribution

As it was previously mentioned, volumes relate the amount of drug with its concentration. Each compartment included in a multi-compartmental model will have its own volume. However, in this section we will refer to the relation between the total drug amount within the body and its concentration in the central compartment.

In the framework of the two-compartment model, right after an intravenous bolus administration, the drug will distribute (instantaneously and uniformly) throughout the central compartment. Therefore, the initial volume of distribution corresponds to the volume of the central compartment, V_1 (sometimes termed V_c), which may be computed as:

$$\frac{D}{C_1 + C_2} = V_1 \tag{26}$$

During the disposition phase, the concentration of the drug in plasma decreases largely owing to the distribution to the peripheral compartment and to the elimination from the central compartment. Henceforth, the volume of distribution increases gradually until it reaches an asymptotic value after the pseudo equilibrium is reached. Such asymptotic value is called the V_{area} (sometimes also denoted V_z or $V_{terminal\ phase}$), which can be computed as:

$$V_{area} = \frac{amount\ of\ drug\ in\ the\ body\ during\ the\ terminal\ phase}{plasma\ concentration\ during\ the\ terminal\ phase} \tag{27}$$

V_{area} owes its name to how it is generally estimated:

$$V_{area} = \frac{D}{AUC_0^{\infty} \beta} = \frac{CL}{\beta} \tag{28}$$

where CL represents plasma drug clearance.

Since V_{area} relies on the drug decay from the body due to its elimination, it is not an adequate volume of distribution in situations for which the amount eliminated is restituted by a continuous input of drug, e.g., at steady state during intravenous infusion.

At steady state, the instantaneous drug input rate exactly compensates the instantaneous elimination rate, and no change in drug plasma levels will be observed as long as the infusion continues at constant rate. In such scenario, the volume of distribution of choice will be the so-called V_{ss} [11]:

$$V_{ss} = \frac{amount\ of\ drug\ in\ the\ body\ at\ steady - state}{plasma\ concentration\ at\ steady - state} \tag{29}$$

V_{area} is invariably larger than V_{ss}, although their difference is generally small.

Regarding practical applications, V_c is rarely used, mostly to predict the initial plasma concentration for an intravenous bolus and anticipate possible safety issues when a loading dose is rapidly given. V_{area} is useful to estimate the remaining amount of drug in the body in the terminal phase, a valuable information in mass balance trials. V_{ss} is relevant to compute loading doses under life-threatening conditions, when achieving steady-state concentrations in an immediate manner is required.

Cross-References

- ▶ Drug Absorption
- ▶ Drug Distribution
- ▶ Drug Excretion
- ▶ Drug Metabolism
- ▶ Linear and Nonlinear Pharmacokinetics
- ▶ One-Compartment Pharmacokinetic Model
- ▶ Real and Apparent Volumes of Distribution

References

1. Schmidt H, Radivojevic A. Enhancing population pharmacokinetic modeling efficiency and quality using an integrated workflow. J Pharmacokinet Pharmacodyn. 2014;41:319–34.
2. Wu X, Nekka F, Li J. Steady-state volume of distribution of two-compartment models with simultaneous linear and saturated elimination. J Pharmacokinet Pharmacodyn. 2016;43:447–59.
3. Abramson FP. Two-compartment pharmacokinetic models: computer simulations of their characteristics and clinical consequences. J Pharm Sci. 1981;70:141–6.
4. Rowland M, Thomson PD, Guichard A, Melmon KL. Disposition kinetics of lidocaine in normal subjects. Ann N Y Acad Sci. 1971;179:383–98.
5. Gibaldi M. Estimation of the pharmacokinetic parameters of the two-compartment open model from post-infusion plasma concentration data. J Pharm Sci. 1969;58:1133–5.
6. Greenblatt DJ, Kock-Weser J. Drug therapy. Clinical pharmacokinetics (first of two parts). N Engl J Med. 1975;293:702–5.
7. Lewis GP, Jusko WJ. Pharmacokinetics of ampicillin in cirrhosis. Clin Pharmacol Ther. 1975;18:475–84.
8. Wagner JG. A safe method for rapidly achieving plasma concentration plateaus. Clin Pharmacol Ther. 1974;16:691–700.
9. Kristensen LO, Weismann K, Hutters L. Renal function and the rate of disappearance of methotrexate from serum. Eur J Clin Pharmacol. 1975;8:439–44.
10. Kristiansen VM, Dewi S, Horsberg TE, Jonasdottir TJ, Moe L, Berlinger B, Lindkaer-Jensen S, Larsen S. Tolerability and pharmacokinetic profile of a novel benzene-poly-carboxylic acids complex with cis-diammineplatinum (II) dichloride in dogs with malignant mammary tumours. Vet Comp Oncol. 2017;15:118–32.
11. Toutain PL, Bousquet-Mélou A. Volumes of distribution. J Vet Pharmacol Ther. 2004;27:441–53.